Development of fluorinated and methoxylated benzothiazole derivatives as highly potent and selective cannabinoid CB2 receptor ligands

Aly, M. W.; Ludwig, F.-A.; Deuther-Conrad, W.; Brust, P.; Abadi, A. H.; Moldovan, R.-P.; Osman, N. A.;

Originally published:

July 2021

Bioorganic Chemistry 114(2021), 105191

DOI: https://doi.org/10.1016/j.bioorg.2021.105191

Fluorinated and methoxylated benzothiazole derivatives as highly affine and selective cannabinoid CB2 receptor ligands.

Mayar W. Aly[1], Friedrich-Alexander Ludwig[2], Winnie Deuther-Conrad[2], Peter Brust[2], Ashraf H. Abadi[1], Rareş-Petru Moldovan[2]*, Noha A. Osman[1]*

[1]Department of Pharmaceutical Chemistry, Faculty of Pharmacy and Biotechnology, German University in Cairo; Egypt

[2] Helmholtz-Zentrum Dresden-Rossendorf, Institute of Radiopharmaceutical Cancer Research, Department of Neuroradiopharmaceuticals, Research Site Leipzig, Leipzig 04318, Germany.

- **To whom correspondences should be addressed, emails: nohaabdelazizosman@gmail.com; noha.osman@guc.edu.eg and r.moldovan@hzdr.de**

Abstract

Numerous studies have indicated the upregulation of the cannabinoid type 2 receptors (CB_2 receptors) under various pathological conditions, and that their visualization with PET could provide a non-invasive diagnostic and/or therapy-monitoring tool in such disorders. Encouraged by promising CB_2 affinity results obtained for a benzothiazole lead compound, **6a**, further structural optimisations were performed which led to the development of a series of fluorinated and methoxylated benzothiazole derivatives, endowed with extremely high CB_2 binding affinity and selectivity, along with structural sites suitable for radiolabeling. Compounds **20**, **21**, **24**, **25**, **29** and **32** displayed CB_2 K_i values in the subnanomolar range (ranging from 0.16 nM to 0.68 nM) and remarkable selectivity for CB_2 over CB_1 (14,000- to 57,000-fold). The fluorinated analogs, **21** and **29**, were evaluated for their in vitro metabolic stability in mouse and human liver microsomes (MLM and HLM). Contrary to the results revealed by studies in HLM, both **21** and **29** displayed a significantly high stability (98% and 91% intact compounds, respectively) after 60 min incubation with MLM.

KEYWORDS

CB_2 ligands, Cannabinoid receptor type 2, Binding affinity, Selectivity, Fluorine, Benzothiazole, Structure activity relationship, Metabolic studies, Positron emission tomography, PET.

ABBREVIATIONS

CB_1, Cannabinoid receptor 1; CB_2, Cannabinoid receptor 2; Et_3N,TEA, triethylamine; rt, room temperature; eq, equivalence; DMF, N,N-dimethylformamide; DCM, Dichloromethane; DMSO, Dimethyl sulfoxide; $CDCl_3$, Deuterated chloroform; EtOAc, Ethyl acetate; MeOH, Methanol; HPLC, high performance liquid chromatography; MS, mass spectrometry; SAR, structure activity relationship; TLC, Thin layer chromatography; NADPH, Nicotinamide adenine dinucleotide phosphate; K_i, Inhibition constant; EC_{50}, 50% effective concentration; SI, selectivity index.

1. Introduction

Our understanding of the endocannabinoid system has greatly improved, over the past two decades, and all that was gratitude to the wealth of results obtained from the immense studies that have been devoted to this research area. The endocannabinoid system is in fact a complex lipid signaling system that is involved in regulating a multitude of physiological processes [(1)] including memory,[(2)] appetite,[(3)] energy balance and metabolism,[(4)] immune function,[(5)] pain sensation,[(6)] and in mediating the pharmacological effects of cannabis.[(7)] Similar to any other physiological system, it is comprised of three key elements which are: endogenous ligands, namely endocannabinoids, receptors and enzymes. The biological processes carried out by the endocannabinoid system, is mediated through two comparable receptors dubbed; central cannabinoid (CB_1) [(8)] and peripheral cannabinoid (CB_2) [(9)] receptors. Both of these receptors belong to the superfamily of heptahelical G-protein coupled transmembrane receptors (GPCRs), [(10)] which were cloned in 1990 and 1993, respectively.[(11)]

CB_1 receptors were found to be more predominant in the central nervous system, meanwhile their concentration is relatively less in the periphery.[12] Unlike the ubiquitous CB_1 receptor, the CB_2 receptors were only detected in very low concentrations in healthy brains and were found to be principally expressed by cells of the immune system.[13,14,15]

It has been evident that the CB_2 receptor is an attractive target for a wide array of therapeutic applications, particularly, where anti-inflammatory and immunomodulatory effects are needed, while eliciting no or minimal psychotropic adverse effects that have plaqued the CB_1-based therapeutics.[16,17]

Moreover, the CB_2 receptor is prominently upregulated under neuroinflammatory conditions including Alzheimer's,[18] Parkinson's,[19] multiple sclerosis,[20] and amyotrophic lateral sclerosis,[21] as well as various cancer types.[22, 23] This protective upregulation can contribute to slower disease progression and symptoms amelioration of such disorders.[24] In addition, the use of CB_2-selective radiotracers for PET imaging of the CB_2 receptor upregulation in neuroinflammation, neurodegeneration and several cancers could offer a promising diagnostic and therapy monitoring tool and also help in improving our understanding of the disease pathogenesis.[25, 26, 27]

In the past years, several ^{11}C- and ^{18}F-labeled CB_2 ligands from diverse chemical scaffolds have been reported, including pyridines,[28] tetrahydrobenzo[b]thiophenes,[27] oxoquinolines,[29,30] thiazoles,[31,32] and indoles.[33,34] (**Figure 1**). A prominent example is the 2-oxoquinoline derivative, [^{11}C]NE40, as it is the first and, to the best of our knowledge, the only CB_2 receptor radioligand to be tested in humans until this date.[29, 35, 36]

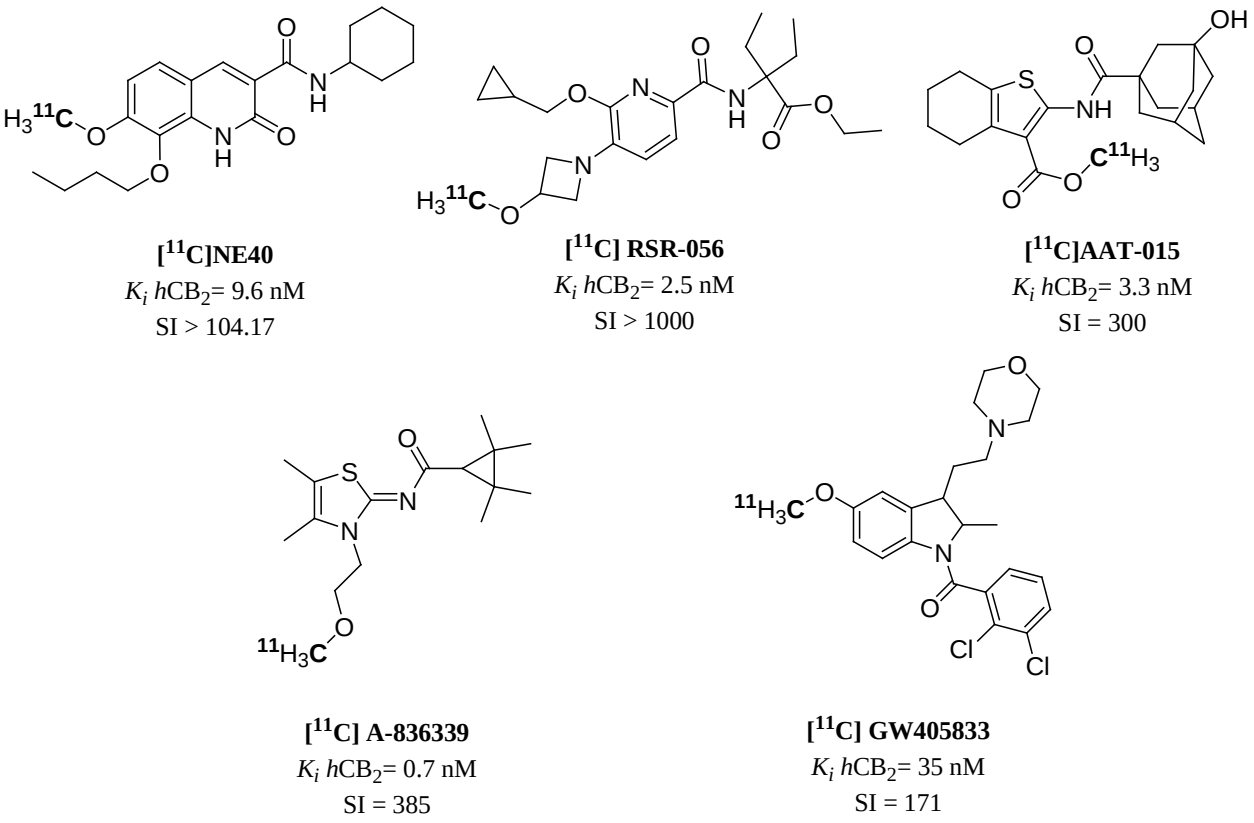

Figure 1: Representative CB_2 radioligands from diverse chemical scaffolds

Despite of the substantial number of CB_2 radioligands that have been specifically developed for this purpose, only a few have made it to clinical trials, while, none has yet been granted approval for use in humans in a clinical setting.[37] The latter has been reported to be attributed to high non-specific binding, production of brain penetrating radiometabolites, prompt metabolism or inappropriate pharmacokinetics.[32] Hence, this has motivated us to focus our efforts on the development of highly affine and selective CB_2 ligands that are eligible for radiolabeling and, thus, have the potential for use as PET tracers.

Recently, our research group has disclosed the medicinal chemistry of a novel benzothiazole-2-ylidine carboxamide series, endowed with high CB_2 receptor binding affinity. Lead compound,

6a (**Figure 2**) exhibited an exceptional CB_2 binding affinity (K_i of 0.10 nM) and an appreciable selectivity to CB_2 over CB_1 receptor (K_i hCB_1/K_i hCB_2 of 120), alongside a full agonistic activity on CB_2 receptors (CB_2 EC_{50} of 26.30 nM).[38] In light of these findings, we were intrigued to conduct further pharmacophore exploration and optimization studies in an effort to enhance its CB_2 selectivity and explore the impact of introducing structural moieties suitable for radiolabeling. Pharmacomodulations, summarized in **Figure 2**, were focused on: the moiety borne by the carboxamide functionality, introducing a methoxy substituent at different positions of the benzothiazole ring and investigating the effect of different *N*3-substituents bearing either a terminal fluorine atom or a methoxy group as sites eligible for radiolabeling.

The present work describes the synthesis of novel fluorinated and methoxylated benzothiazole-based CB_2 ligands, as a precondition for the development of an effective radiotracer for CB_2 receptors imaging with PET. The newly synthesized derivatives were tested in competitive radioligand binding assays towards hCB_1 and hCB_2 receptors overexpressed on membranes of CHO cell lines and affinity data were used for calculation of their CB_2 selectivity. Based on the new SAR findings, hit compounds were subjected to in vitro metabolic studies in mouse and human liver microsomes to assess their metabolic stability.

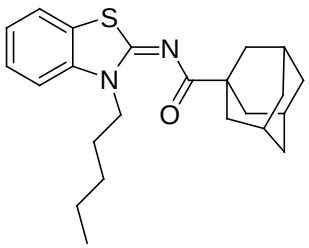

Hit compound **6a**
*h*CB$_2$ K_i = 0.10 nM
*h*CB$_1$$K_i$ = 12.38 nM
SI (k_i *h*CB$_1$/ k_i *h*CB$_2$) = 120

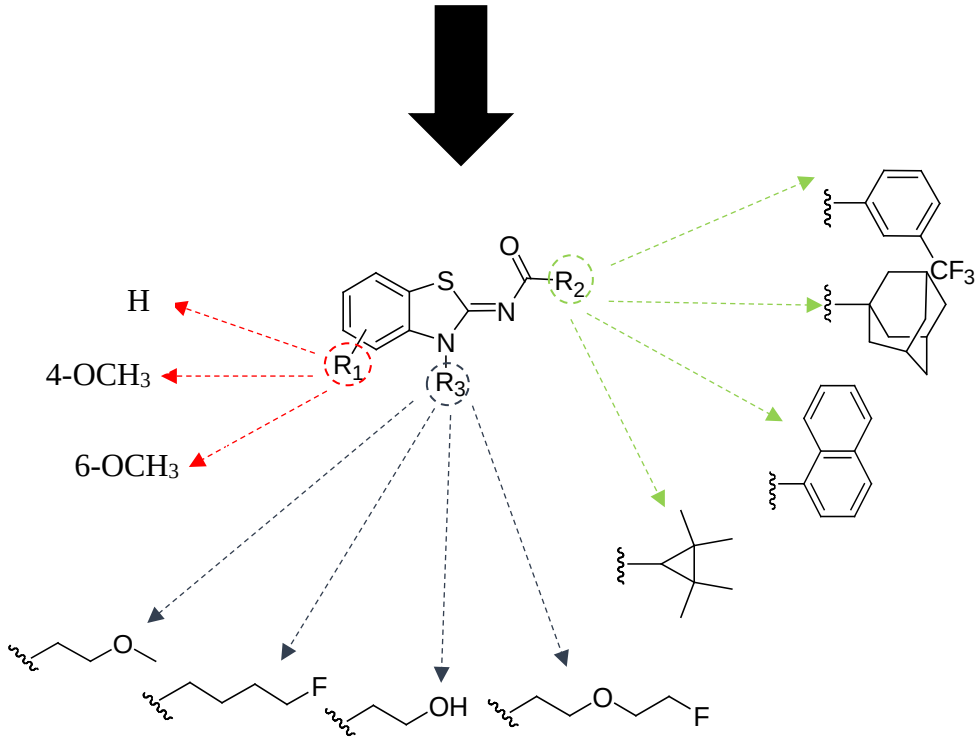

Figure 2: Structural variations adopted on lead compound **6a**

2. Results and discussion

2.1. Chemistry

The synthesis of the desired [*N*-(3-substituted)-4-/6-methoxy/unsubstituted-3*H*-benzothiazol-2-ylidene] carboxamide **(**compounds **14-33)** was accomplished via the steps outlined in **Scheme 1**. The procedure generally illustrates two steps; first a coupling reaction between acyl chlorides or carboxylic acids and compounds **1-3** to afford the corresponding **4-13** carboxamides, followed

by alkylation of position 3 of the benzothiazole ring of the latter derivatives to introduce a site suitable for radiolabelling and thus, yield the corresponding **14-33** ylidene derivatives. Amide coupling has been carried out using two different methods (**a** and **b**) depending on the available starting materials. **Method a** involved the reaction between the commercially available 2-aminobenzothiazole and different acid chlorides to synthesise compounds **4-10**. This reaction was carried out under inert conditions using triethylamine (TEA) as a base, to form a nucleophile out of the 2-aminobenzothiazole, in DCM for about 18-24 hours.

On the other hand, **method b** was utilised to couple carboxylic acids to amines using BOP (benzotriazole-1-yloxy)tris(dimethylamino)phosphonium hexafluorophosphate), as a coupling agent, to give compounds **11-13**. In this case, the reactions were started in DCM, at 0 °C followed by stirring at room temperature for 24 hours.

The alkylation step was carried out using sodium hydride (NaH), which acts as a base, in order for the alkylation reaction to take place. NaH was first allowed to stir with the *N*-(benzothiazol-2-yl) carboxamide derivative, in dry DMF, for 1 hour, after which different alkyl bromides were added. The optimum reaction time was 24 hours, allowing the reaction to give the best yield (60-80%), with minimal impurities which were removed by column chromatography.

As outlined in **Scheme 2**, 3-(2-hydroxyethyl)-2-aminobenzothiazole derivatives, **34** and **35,** were synthesized through alkylating differently substituted 2-aminobenzothiazoles (**1** and **2**) with 2-bromoethan-1-ol in a sealed vessel, under neat conditions, at 90°C. The resulted residue was used in the following step without further purification. **34** and **35** were then coupled with 2,2,3,3-tetramethylcyclopropane-1-carboxylic acid using BOP to yield the corresponding amides,

36 and **37**. The hydroxyl group of the latter compound (**37**) was then subjected to alkylation with 1-fluoro-2-iodoethane, using NaH, in dry DMF to afford compounds **38**.

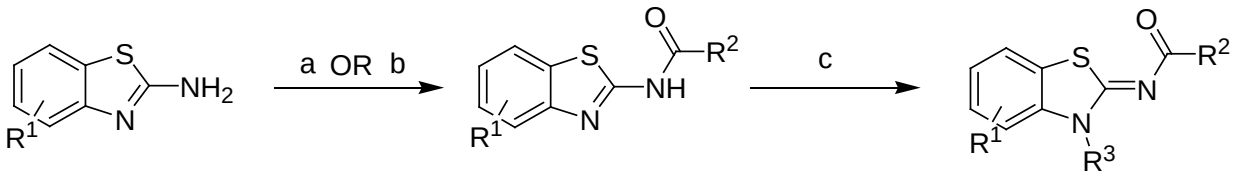

1-3 **4-13** **14-33**

1: R^1=H
2: R^1=4-OCH_3
3: R^1=6-OCH_3
4: R^1=H; R^2= 3-trifluorophenyl
5: R^1=4-OCH_3; R^2= 3-trifluorophenyl
6: R^1=6-OCH_3; R^2= 3-trifluorophenyl
7: R^1=H; R^2= adamantan-1-yl
8: R^1=4-OCH_3; R^2=adamantan-1-yl
9: R^1=6-OCH_3; R^2= adamantan-1-yl
10: R^1=H; R^2= naphth-1-yl
11: R^1=H; R^2= 2,2,3,3-tetramethylcyclopropane-1-yl
12: R^1=4-OCH_3; R^2= 2,2,3,3-tetramethylcyclopropane-1-yl
13: R^1=6-OCH_3; R^2= 2,2,3,3-tetramethylcyclopropane-1-yl
14: R^1=H; R^2= 3-trifluorophenyl; R^3= 2-methoxyethtyl
15: R^1=H; R^2= 3-trifluorophenyl; R^3= 4-fluorobutyl
16: R^1=4-OCH_3; R^2= 3-trifluorophenyl; R^3= 2-methoxyethtyl
17: R^1=4-OCH_3; R^2= 3-trifluorophenyl; R^3= 4-fluorobutyl
18: R^1=6-OCH_3; R^2= 3-trifluorophenyl; R^3=2-methoxyethtyl
19: R^1=6-OCH_3; R^2= 3-trifluorophenyl; R^3= 4-fluorobutyl
20: R^1=H; R^2= adamantan-1-yl; R^3=2-methoxyethtyl
21: R^1=H; R^2= adamantan-1-yl; R^3=4-fluorobutyl
22: R^1=4-OCH_3; R^2=adamantan-1-yl; R^3=2-methoxyethtyl
23: R^1=4-OCH_3; R^2=adamantan-1-yl; R^3=4-fluorobutyl
24: R^1=6-OCH_3; R^2= adamantan-1-yl; R^3=2-methoxyethtyl
25: R^1=6-OCH_3; R^2= adamantan-1-yl; R^3=4-fluorobutyl
26: R^1=H; R^2= naphth-1-yl; R^3=2-methoxyethtyl
27: R^1=H; R^2= naphth-1-yl; R^3=4-fluorobutyl
28: R^1=H; R^2= 2,2,3,3-tetramethylcyclopropane-1-yl; R^3=2-methoxyethtyl
29: R^1=H; R^2= 2,2,3,3-tetramethylcyclopropane-1-yl; R^3=4-fluorobutyl
30: R^1=4-OCH_3; R^2= 2,2,3,3-tetramethylcyclopropane-1-yl; R^3=2-methoxyethtyl
31: R^1=4-OCH_3; R^2= 2,2,3,3-tetramethylcyclopropane-1-yl; R^3=4-fluorobutyl
32: R^1=6-OCH_3; R^2= 2,2,3,3-tetramethylcyclopropane-1-yl; R^3=2-methoxyethtyl
33: R^1=6-OCH_3; R^2= 2,2,3,3-tetramethylcyclopropane-1-yl; R^3=4-fluorobutyl

Scheme 1. Synthesis of [*N*-(3-substituted)-4-/6-methoxy/unsubstituted-3*H*-benzothiazol-2-ylidene] carboxamide derivatives; **14-33**. Reagents and conditions: (a) 1 eq. 2-

aminobenzothiazole, 1.5 eq. Et_3N, 1.5 eq. acyl chloride, DCM, 0 °C to rt, 18-24 h. (b) 1 eq. 2-aminobenzothiazole, 1 eq. 2, 2, 3, 3-tetramethylcyclopropane-1-carboxylic acid, 3 eq. Et_3N, 1.3 eq. BOP, DCM, 0 °C to rt, 24 h (c) 1.3 eq. of the appropriate *N*-(benzothiazol-2-yl) carboxamide, 1.9 eq. NaH, 1.4 eq. appropriate alkyl bromide, DMF, rt 1 h, 80 °C overnight.

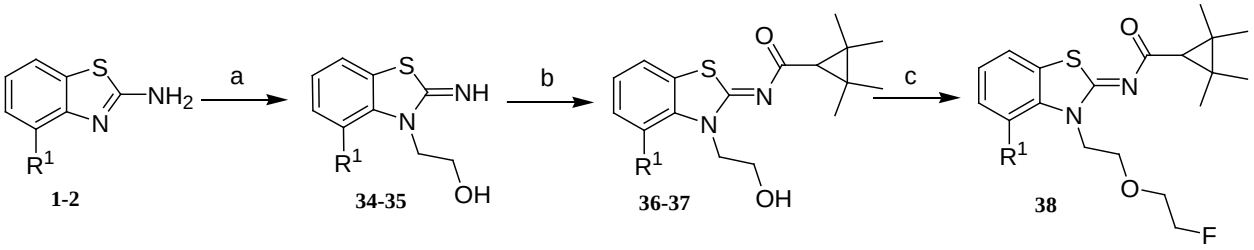

1: R^1= H
2: R^1= 4-OCH_3
34, 36: R^1=H
35, 37, 38: R^1=4-OCH_3

Scheme 2. Synthesis of *N*-{3-[2-(2-Fluoroethoxy)-ethyl]-4-methoxy-3*H*-benzothiazol-2-ylidene}-2,2,3,3-tetramethyl-cyclopropyl-carboxamide **38**. Reagents and conditions: (a) 1 eq. 2-aminobenzothiazole, 1.5 eq. bromoethan-1-ol, sealed vessel, neat, 90°C, 16-24 h (b) 1 eq. 3-alkylated-2-aminobenzothiazole, 1 eq. 2,2,3,3-tetramethylcyclopropane carboxylic acid, 3 eq. Et_3N, 1.3 eq. BOP, DCM, 0 °C to rt, 24 h (c) 1 eq. of alcoholic solution of **37**, 3 eq. NaH in DMF at rt, 5 min, 5 eq. 1-fluoro-2-iodoethane, rt, 20-24 h.

2.2. Structure-activity relationships

Newly synthesized compounds were evaluated in radioligand binding assays for their ability to displace [^{3}H]-WIN-55,212-2 (a high affinity radioligand; K_D = 3.3 nM for CB_2 receptor) from human recombinant CB_2 receptors and to displace [^{3}H]SR141716A (K_D = 2.3 nM for CB_1 receptor) from human recombinant CB_1 receptors. Binding assays were done for compounds, generating IC_{50} values. K_i values were calculated by applying the Cheng-Prusoff equation to the IC_{50} values, whenever possible. The obtained data are shown in **Table 1**.

In the first round of structural modifications, two positions were investigated; the effect of different amide substituents (R^2) and different *N*3-substituents (R^3). It can be generally deduced that the nature of the amide substituent greatly influences the CB_2 binding affinity and selectivity of the synthesized compounds. For compounds with a 4-fluorobutyl chain as R^3, it was evident that having an adamantyl amide moiety provided the most superior CB_2 binding affinity and selectivity over CB_1 (**21**, K_i = 0.28 nM, SI = 21,614). Interchanging the adamantyl with a smaller, more strained 2,2,3,3-tetramethylcyclopropyl ring (**29**) led to an observed drop in affinity and selectivity, however, still retaining a subnanomolar affinity (K_i = 0.51 nM). In efforts to achieve chemical diversity, the effect of aromatic amide substituents was also envisaged. Further decline in the CB_2 affinity and selectivity was noted for the 3-trifluoromethylphenyl amide (**15**, K_i = 29.8 nM, SI = 1759), while the least CB_2 affinity and selectivity, of this series, was displayed by the 1-naphthyl amide derivative (**27**, K_i = 40.7 nM, SI = 109). Based on these findings, it was clear that bulky aliphatic amide substituents are generally favoured over aromatic ones. Upon replacing the *N*3-substituent, 4-fluorobutyl, of (**21**), (**29**), (**15**) and (**27**) with a 2-methoxyethyl group to obtain their respective analogs: (**20**), (**28**), (**14**), and (**26**); the same trend for their CB_2 binding affinity and selectivity was observed (K_i = 0.48, 1.67, 84.2 and 502 nM, respectively).

For the *N*3-substituent, it was generally noticed that a 4-fluorobutyl moiety resulted in a higher CB_2 binding affinity and selectivity over CB_1 versus the 2-methoxyethyl group. This is exemplified by the improvement in binding affinity and selectivity when the 2-methoxyethyl group (**20**) (K_i = 0.48 nM, SI = 14,643) was replaced with the 4-fluorobutyl group (**21**) (K_i = 0.28 nM, SI = 21,614), where the latter is considered as the most affine compound in this series, possessing an optimal selectivity to CB_2 over CB_1 receptors. A similar CB_2 affinity profile was

revealed by the 1-naphthyl amides, (**26**) (K_i = 502 nM) and (**27**) (K_i = 40.7 nM), nevertheless, this was not observed for their CB_2/CB_1 selectivity, where the selectivity was almost halved (SI = 246 and 109, respectively).

Subsequent round of SAR studies was focused on exploring the effect of a phenyl methoxy substituent (R^1) on the binding affinity and selectivity of the present scaffold. Based on the fact that a phenyl methoxy group is a promising pharmacophore of various CB_2 receptor ligands, two new series of compounds were synthesized; the first series functionalized a 6-methoxy group on the 2-aminobenzothiazole scaffold while the second one functionalized it at position 4. These positions were also selected in line with data previously reported in literature. [39]

Interestingly, introducing a 6-methoxy substituent to the *N*3-(4-fluorobutyl)adamantyl amide derivative, **21** (SI = 21,614), afforded compound **25** (SI = 45,578) with a 2-fold greater CB_2 selectivity, while, only a slight decrease in its CB_2 binding affinity (K_i = 0.28 nM vs 0.38 nM). Furthermore, a dramatic increase in the CB_2 binding affinity of the 2,2,3,3-tetramethylcyclopropyl amide (**28**) (K_i = 1.67 nM) was observed when a 6-methoxy moiety was employed giving rise to the more affine counterpart; (**32**) (K_i = 0.16 nM). Worth noting, compound **32** also exhibited a tremendous amplification in its CB_2/CB_1 selectivity (SI = 57,231) compared to **28** (SI = 8604).

To our surprise, applying the same modification to compound **29**, the *N*3-(4-fluorobutyl) analog of **28**, led to a complete loss in affinity to the CB_2 receptor (**33**), representing the only exception to the common trend observed within the 6-methoxylated series. Substituting a 6-methoxy moiety on the *N*3-(4-fluorobutyl)trifluoromethyl phenyl amide (**15**) (K_i = 29.8 nM) yielded compound **19** with a concomitant enhancement in its CB_2 binding affinity (K_i = 11.0 nM). As

successfully anticipated, a similar effect was noted when comparing their *N*3-2-methoxyethtyl analogs, (**14**) and (**18**), respectively.

On the other hand, a 4-methoxy substituent resulted in a series with a generally reduced CB_2 binding affinity. This was evident by comparing the K_i values of the adamantly amides; **20** to **22** (45-fold drop) and **21** to **23** (11-fold drop). Consistently, a 28-fold decline in the CB_2 affinity was observed upon substituting the 3-trifuoromethylphenyl amide derivative (**15**) with a 4-methoxy moiety (compound **17**).

It is worth mentioning that the 2,2,3,3-tetramethylcyclopropyl amide derivatives, **30** and **31**, displayed only a slight drop (approximately 3-fold) in comparison to their 4-methoxy-lacking counterparts, **28** and **29**, respectively. The majority of compounds in this series also demonstrated relatively lower CB_2/CB_1 selectivity profiles compared to the unsubstituted phenyl series.

Table 1. Binding affinities (K_i values) of synthesized compounds towards *h*CB_2 and *h*CB_1 cannabinoid receptors, selectivity indices (K_i *h*CB_1/K_i *h*CB_2).

Cpd	Structure	CB_2 IC_{50} in nM	CB_2 K_i in nM	CB_1 IC_{50} in nM	CB_1 K_i in nM	Selectivity index (SI)
14	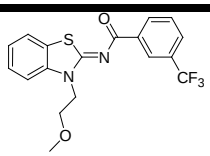	111	84.2	176800	65410	776
15	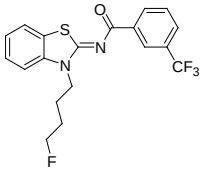	39.4	29.8	141800	52440	1759

16	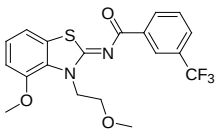	8266	3058	>1000	-	-
17	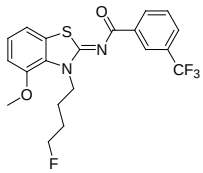	2280	843	>1000	-	-
18	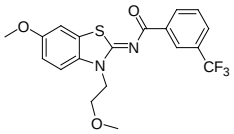	110	54.2	52870	19150	353
19	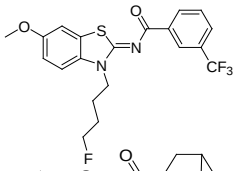	22.5	11.0	>1000	-	-
20	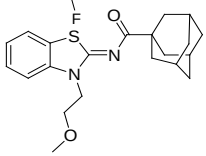	0.64	0.48	19000	7029	14643
21	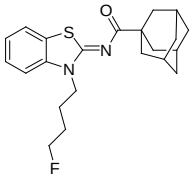	0.37	0.28	16360	6052	21614
22	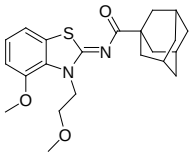	59.2	21.9	167400	74910	3420
23	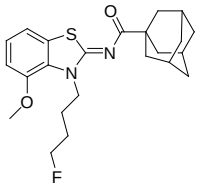	8.17	3.02	41710	18660	6178
24	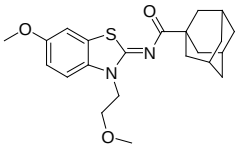	1.84	0.68	88520	-	-
25	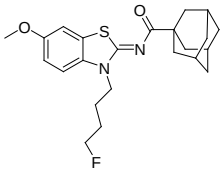	0.77	0.38	38710	17320	45578

26	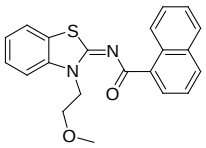	665	502	334900	123900	246
27	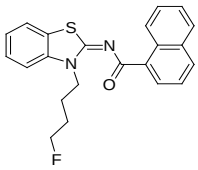	53.8	40.7	12010	4444	109
28	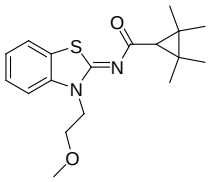	2.21	1.67	38860	14370	8604
29	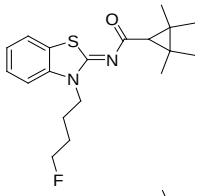	0.67	0.51	14630	5412	10611
30	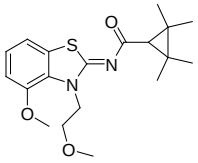	13.3	4.92	>1000	-	-
31	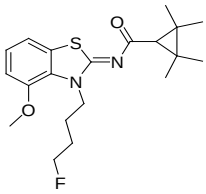	3.83	1.42	1.918 x10^{20}	8.581x 10^{19}	6.06 x10^{19}
32	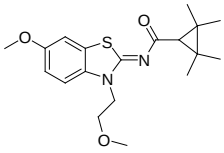	0.44	0.16	25280	9157	57231
33	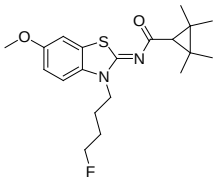	>1000	-	38030	13780	-
36	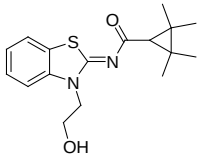	160	59.3	67270	-	-

37	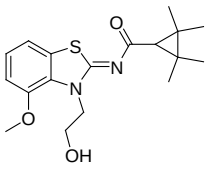	297	-	$5.2030x10^{25}$	-	-
38	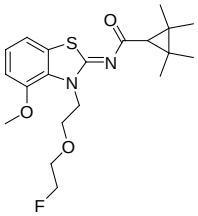	-	-	134600	-	-

2.3. In vitro metabolic studies

Two of the most potent compounds, **21** and **29**, were selected for additional in vitro studies to assess their stability and how prone they are to metabolic degradation. Compounds **21** and **29** (20µM) were incubated with either Mouse Liver Microsomes (MLM) or Human Liver Microsomes (HLM), in the presence of NADPH, at 37°C . Two time points were investigated to assess the intensity of the intact compound; after incubation for 30 min and 60 min. After protein precipitation, which was done by the addition of acetonitrile and subsequent centrifugation, the supernatants were analyzed by HPLC-UV-MS.

2.3.1. Microsomal depletion of **21** and **29**

HPLC-UV-MS charts of the tested compounds at different time points were first compared to negative controls. This was carried out to eliminate any peak that could be due to anything else other than the metabolism of the compound under investigation.

In accordance to the obtained data represented in **Figure 3**, **Figure 4**, **Figure 5** and **Figure 6**; the % intact compound **21**, after 30 min and 60 min incubation with MLM, was found to be 96.73% and 98.34%, respectively. Comparably, 94.57% and 90.77% of **29** remained intact after 30 min and 60 min incubation with MLM, respectively. Thus, it is clear that both compounds

exhibited an exceptionally high metabolic stability in mice. In an effort to validate whether this conclusion also applies to humans, the same experiments were carried out but using HLM in place of MLM.

Surprisingly, only 24.39% and 18.23% of the parent compound **21** remained intact, after 30 min and 60 min incubation, respectively, demonstrating a dramatic decrease in its metabolic stability when incubated with HLM vs MLM. In a similar trend, 49.60% and 31.98% unmetabolised **29** were detected when subjected to the same conditions. Hence, it's obvious that studies in MLM do not, necessarily, mirror the real picture in HLM, emphasising the importance of carrying out metabolic studies in HLM, as a prerequisite to choosing a credible lead compound for further optimisations. The obtained percentages also reveal that replacing the adamantly amide substituent (in **21**) with a 2,2,3,3-tetramethylcyclopropyl amide (in **29**) was accompanied by a significant increase in the metabolic stability for **29** (2-fold and 1.75-fold higher % intact compound at 30 and 60 min, respectively). This observation could be attributed to the greater steric hindrance provided by the 2,2,3,3-tetramethyl substituents at the cyclopropyl ring.

2.3.2. Identification of in vitro metabolites

Looking at **Figure 3**, a total of 7 metabolites of compound **21** were detected, after 30 min and 60 min of incubation with HLM. On the other hand, **Figure 5** displays a total of 8 and 10 metabolites of compound **29** after 30 min and 60 min incubation, respectively, where only one is considered as a major metabolite, exhibiting an average of 23.99% after 30 min incubation. The latter corresponds to the peak at R_t of 8.25 and displays a M.Wt of 379.16 $(M+H)^+$. Suggested metabolite structure is provided in **Figure 7**, which could be formed via the defluorinaton of the

N-alkyl chain followed by hydroxylation, in addition to, thiazole sulphur oxidation to yield the sulphonyl derivative.

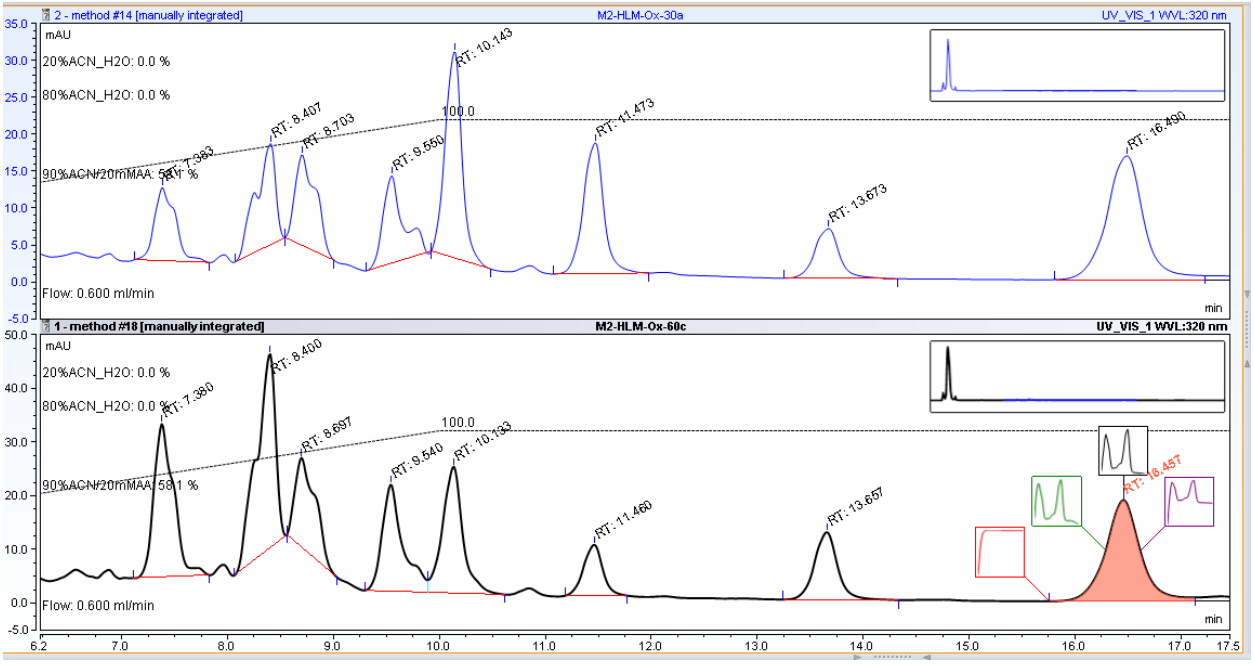

Figure 3. HPLC-UV chromatogram of compound **21** after incubation for 30 min (upper graph) and 60 min (lower graph), in HLM. The peaks indicated with a red baseline, designates metabolites produced from each of the incubated compounds. Peak with R_t = 16.4 represents the parent compound.

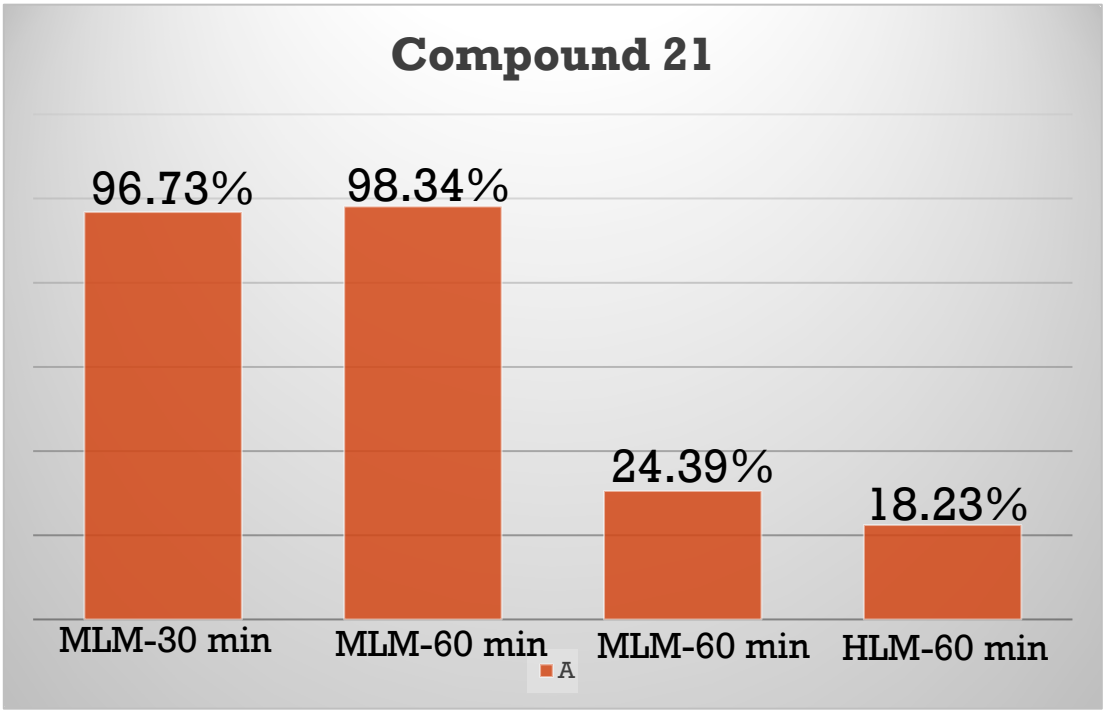

Figure 4. Bar chart representing the percent concentration of intact compound **21** obtained after incubation for 30 min and 60 min in MLM and HLM.

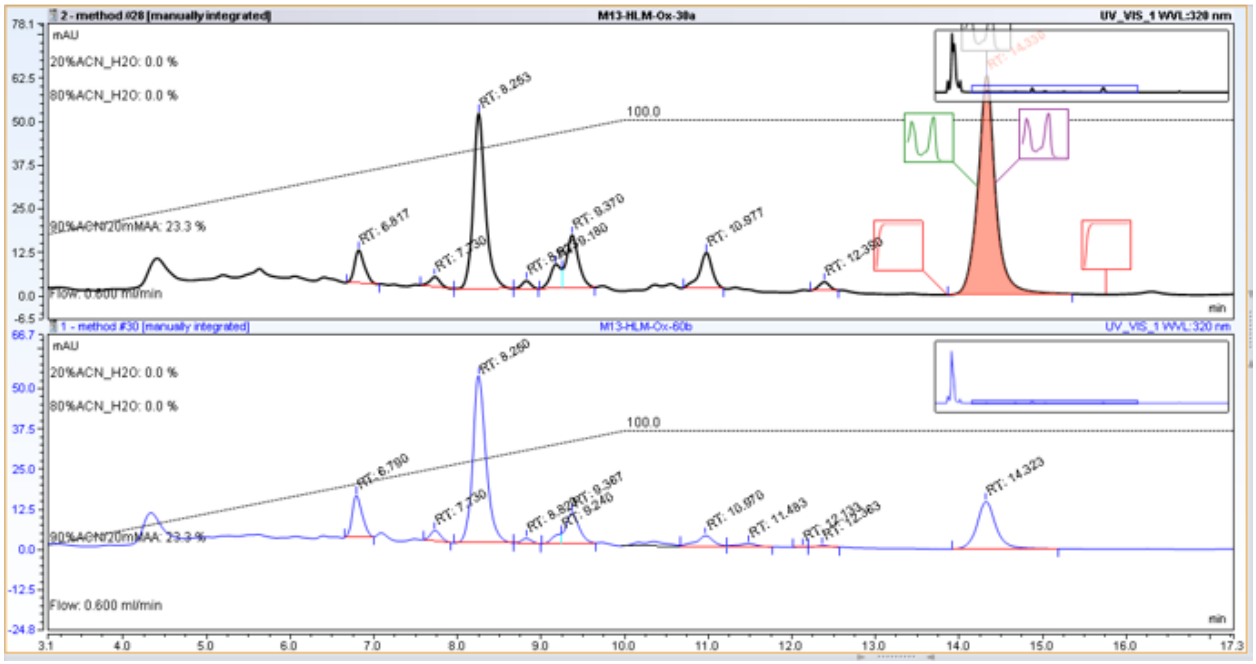

Figure 5. HPLC-UV chromatogram of compound **29** after incubation for 30 min (upper graph) and 60 min (lower graph) in HLM. The peaks indicated with a red baseline, designates metabolites produced from each of the incubated compounds. Peak with R_t = 14.3 represents the parent compound.

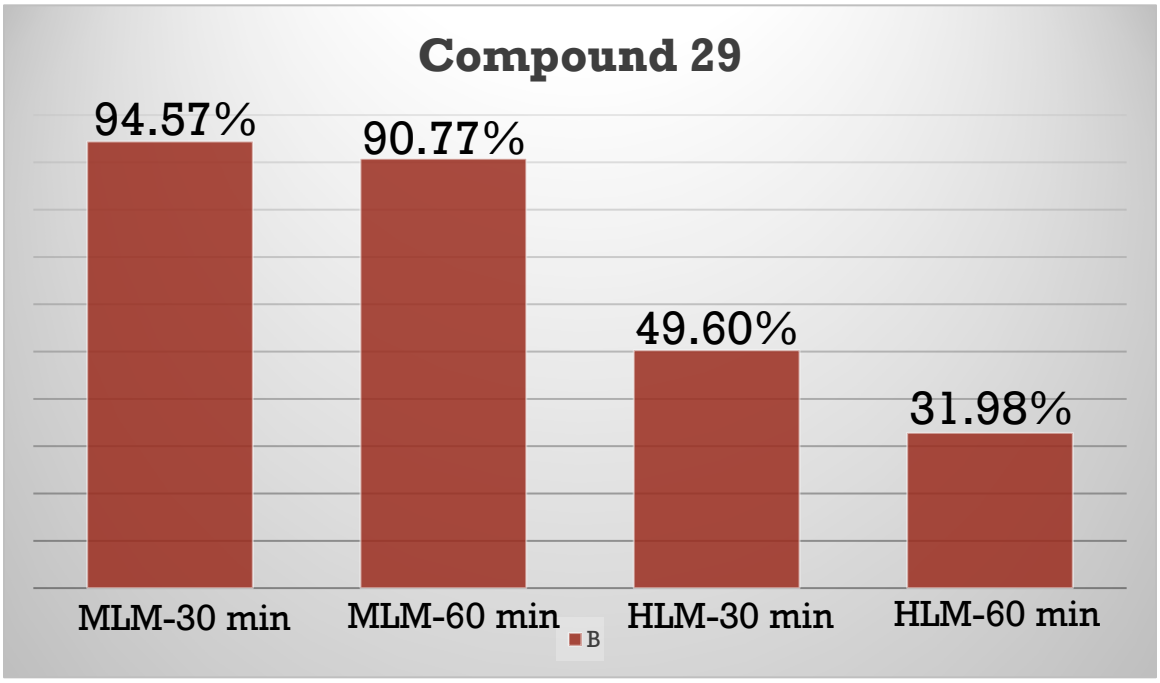

Figure 6. Bar chart representing the percent concentration of intact compound **29** obtained after incubation for 30 min and 60 min in MLM and HLM.

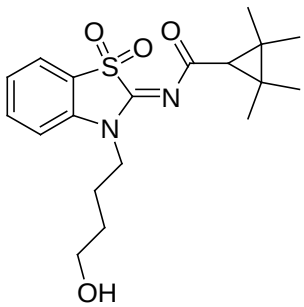

Mwt: 379.16 $(M+H)^+$

Figure 7. Compound **29** major metabolite

3. Experimental section

Chemistry. Solvents and reagents were obtained from commercial suppliers and were used without further purification. All organic solvents used were of pure analytical or HPLC grade. Column chromatography was carried out using silica-gel 40-60 µm mesh with DCM, DCM/MeOH, Hexane/EtOAc, Hexane/DCM, Heptane/EtOAc, DCM/Acetone mixtures as eluents. Reaction progress was monitored by TLC using fluorescent pre-coated silica gel plates and detection of the components was made by short UV light (λ= 254 nm). ^{1}H-NMR, ^{13}C-NMR spectra were recorded at 400 MHz using Varian Mercury 400 Plus and at 300 MHz using Varian 300 MHz spectrometer. ^{1}H shifts are referenced to the residual protonated solvent signal (δ 2.50 for DMSO-*d*$_6$ and δ 7.26 for $CDCl_3$) and ^{13}C shifts are referenced to the deuterated solvent signal (δ 39.5 for DMSO-*d*$_6$ and δ 77.0 for $CDCl_3$). Chemical shifts are given in parts per million (ppm), and all coupling constants (*J*) are given in Hz. The purities of the tested compounds were determined by HPLC coupled with mass spectrometry and were higher than 95% purity for all final compounds.

Mass spectrometric analysis (UPLC-ESI-MS) was performed using Waters ACQUITY Xevo TQD system, which consisted of an ACQUITY UPLC H-Class system and Xevo^{TM}TQD triple-quadrupole tandem mass spectrometer with an electrospray ionization (ESI) interface (Waters Corp., Milford, MA, USA). Acquity BEH C_{18}100 mm × 2.1 mm column (particle size, 1.7 µm) was used to separate analytes (Waters, Ireland). The solvent system consisted of water containing 0.1% TFA (A) and 0.1% TFA in acetonitrile (B). HPLC-method: flow rate 200 µL/min. The percentage of B started at an initial of 5% and maintained for 1 minute, then increased up to 100% during 10 min, kept at 100% for 2 min, and flushed back to 5% in 3 min. The MS scan was carried out at the following conditions: capillary voltage 3.5 kV, cone voltage

20V, radio frequency (RF) lens voltage 2.5V, source temperature 150 °C and desolvation gas temperature 500 °C. Nitrogen was used as the desolvation and cone gas at a flow rate of 1000 and 20 L/h, respectively. System operation and data acquisition were controlled using Mass Lynx 4.1 software (Waters).

High resolution mass spectrometric analysis (HR-ESI-MS) was performed using Bruker micrOTOF-Q II instrument or Impact II Bruker Daltonics. For the former exact masses were obtained in 4 decimal places, while the latter obtained the exact masses in 5 decimal places. They were acquired in a positive mode and data are reported as m/z. All masses were reported either as $(M+H)^+$, $(M+Na)^+$ or $(M+Cu)^+$. Melting points were determined on BuchiB-540 Melting Point apparatus and are uncorrected. All reactions were carried out under argon when inert atmosphere was needed.

3.1. General synthetic methods and experimental details

3.1.1. Procedure for the synthesis of of *N*-(4-/6-Methoxy/unsubstituted-benzothiazol-2-yl) carboxamide derivatives (4-10)

The appropriate acyl chloride (1.5 mmol) was slowly added under inert atmosphere to a cooled (0 °C) solution of 2-aminobenzothiazole (1 mmol) and TEA (1.5 mmol) in dry DCM (10 mL). After being stirred at room temperature for 18-24 h, the solution was washed with 1 N HCl, saturated solution of $NaHCO_3$ and brine, then dried over anhydrous $MgSO_4$ and evaporated to dryness. The crude product was further purified using column chromatography.

***N*-Benzothiazol-2-yl-3-trifluoromethyl-benzamide (4)** [38] White crystals, 79.65%; mp: 211-212°C; MS (ESI): m/z 323.1 $(M+H)^+$.

***N*-(4-Methoxy-benzothiazol-2-yl)-3-trifluoromethyl-benzamide (5)** Yellow powder,69.43%; mp**:** 179-181°C; MS (ESI): *m/z* 353.1 $(M+H)^+$; HRMS (ESI): *m/z* 767.02119, calcd 767.03826 for $C_{32}H_{22}CuF_6N_4O_4S_2$ $(2M+Cu)^+$; ^{1}H-NMR (δ): (400 MHz, $CDCl_3$) δ 12.11 (s, 1H), 8.23 (s, 1H), 8.08 (d, *J* = 7.8 Hz, 1H), 7.75 (d, *J* = 7.8 Hz, 1H), 7.45-7.43 (m, 2H), 7.27 (t, *J* = 8.0 Hz, 1H), 6.70 (d, *J* = 8.0 Hz, 1H), 3.52 (s, 3H); ^{13}C-NMR (δ): (101 MHz, $CDCl_3$) δ 164.70, 158.67, 151.50, 137.63, 133.26, 133.15, 131.50, 131.17, 131.02, 129.22, 125.27, 125.06 (q, $^3J_{CF}$ = 3.9 Hz), 123.34 (q, $^1J_{CF}$ = 272.9 Hz), 113.45, 106.53.

***N*-(6-Methoxy-benzothiazol-2-yl)-3-trifluoromethyl-benzamide (6)** Yellowish powder, 78.64%; mp: 201-203°C; MS (ESI): *m/z* 353.1 $(M+H)^+$; HRMS (ESI): *m/z* 767.02053, calcd 767.03826 for $C_{32}H_{22}CuF_6N_4O_4S_2$ $(2M+Cu)^+$; ^{1}H-NMR (δ): (400 MHz, $CDCl_3$) δ 12.11 (s, 1H), 8.24 (s, 1H), 8.15 (d, *J* = 7.9 Hz, 1H), 7.78 (d, *J* = 8.6 Hz, 1H), 7.55 (dt, *J* = 25.1, 7.8 Hz, 1H), 7.32 (d, *J* = 2.5 Hz, 1H), 7.03 (d, *J* = 8.9 Hz, 1H), 6.84 (dd, *J* = 8.9, 2.5 Hz, 1H), 3.87 (s, 3H); ^{13}C-NMR (δ): (101 MHz, $CDCl_3$) δ 173.17, 167.32, 156.85, 137.51, 132.52, 131.20, 130.54 (q, $^2J_{CF}$ = 32.4 Hz), 128.62, 128.11 (q, $^3J_{CF}$ = 3.7 Hz), 127.77, 126.28 (q, $^3J_{CF}$ = 3.9 Hz), 128.94 – 119.80 (q, $^1J_{CF}$ = 292.9), 115.03, 113.27, 106.31.

***N*-(Benzothiazol-2-yl)-adamantyl-carboxamide (7)** [38] White powder, 78.98%; mp: 191-193°C; MS (ESI): *m/z* 313.2 $(M+H)^+$.

***N*-(4-Methoxy-benzothiazol-2-yl)-adamantyl-carboxamide (8)** White powder, 72.09%; mp: 178-179°C; MS (ESI): *m/z* 343.2 $(M+H)^+$; HRMS (ESI): *m/z* 747.20509 calcd 747.21999 for $C_{38}H_{44}CuN_4O_4S_2$ $(2M+Cu)^+$; ^{1}H-NMR (δ): (400 MHz, $CDCl_3$) δ 9.16 (s, 1H), 7.37 (d, *J* = 8.0 Hz, 1H), 7.22 (t, *J* = 8.0 Hz, 1H), 6.85 (d, *J* = 7.9 Hz, 1H), 3.99 (s, 3H), 2.08 (s, 3H), 1.94 (d, *J* =

2.4 Hz, 6H), 1.73 (q, *J* = 12.3 Hz, 6H); ^{13}C-NMR (δ): (101 MHz, $CDCl_3$) δ 175.85, 156.93, 151.98, 138.21, 133.62, 124.65, 113.46, 106.60, 55.80, 41.20, 38.83, 36.23, 27.86.

***N*-(6-Methoxy-benzothiazol-2-yl)-1-adamantyl-carboxamide (9)** [40] White powder, 73.41%; mp: 218-219°C; MS (ESI): *m/z* 343.2 $(M+H)^+$.

***N*-(Benzothiazol-2-yl)-1-naphthyl-carboxamide (10)** [38] White powder, 83.17%; mp: 207-208°C; MS (ESI): *m/z* 305.1 $(M+H)^+$.

3.1.2 Procedure for the synthesis of *N*-(4-/6-Methoxy/unsubstituted-benzothiazol-2-yl)-2,2,3,3-tetramethyl-cyclopropyl-carboxamide derivatives (11-13)

2, 2, 3, 3-tetramethylcyclopropane acid (1 mmol), TEA (3 mmol) and BOP (1.3 mmol,) were added to the 2-aminobenzothiazole (1 mmol) in DCM at 0 °C , then the mixture was stirred at room temperature for 24 hours. The reaction was quenched with iced water and extracted with ethyl acetate. The reaction was quenched by addition of 2 mL water followed by a 10 mL aqueous saturated solution of $NaHCO_3$ and 15 mL EtOAc. The phases were separated and the aqueous phase was washed with 2x10 mL ethyl acetate. The combined organic fractions were washed with 20 mL brine, dried over $MgSO_4$ and concentrated by rotary evaporation. The obtained residue was purified by column chromatography.

***N*-(Benzothiazol-2-yl)-2,2,3,3-tetramethyl-cyclopropyl-carboxamide (11)** White powder**,** 82.67%; mp: 190-191°C; MS (ESI): *m/z* 275.2 $(M+H)^+$; HRMS (ESI): *m/z* 611.15222 calcd 611.16756 for $C_{30}H_{36}CuN_4O_2S_2$ $(2M+Cu)^+$; ^{1}H-NMR (δ): (400 MHz, $CDCl_3$) δ 11.40 (s, 1H), 7.79 (dd, *J* = 13.7, 7.9 Hz, 2H), 7.44 – 7.38 (m, 1H), 7.32 – 7.27 (m, 1H), 1.34 (s, 6H), 1.12 (s, 1H), 1.05 (s, 6H); ^{13}C-NMR (δ): (101 MHz, $CDCl_3$) δ 170.60, 159.89, 147.82, 131.76, 126.04, 123.67, 121.48, 120.48, 37.56, 23.45, 16.58.

***N*-(4-Methoxy-benzothiazol-2-yl)-2,2,3,3-tetramethyl-cyclopropyl-carboxamide (12)** White powder, 80.75%; mp: 198-199°C; MS (ESI): *m/z* 305.2 $(M+H)^+$; HRMS (ESI): *m/z* 327.11374 calcd 327.11431 for $C_{16}H_{20}N_2NaO_2S$ $(M+Na)^+$; ^{1}H-NMR (δ): (400 MHz, $CDCl_3$) δ 10.26 (s, 1H), 7.37 (d, *J* = 8.0 Hz, 1H), 7.23 (d, *J* = 8.0 Hz, 1H), 6.88 (d, *J* = 8.0 Hz, 1H), 3.99 (s, 3H), 1.37 (s, 1H), 1.31 (s, 6H), 1.11 (s, 6H); ^{13}C-NMR (δ): (101 MHz, $CDCl_3$) δ 170.08, 157.81, 151.50, 136.85, 132.72, 124.70, 113.44, 106.94, 55.81, 37.81, 23.43, 16.65.

***N*-(6-Methoxy-benzothiazol-2-yl)-2,2,3,3-tetramethyl-cyclopropyl-carboxamide (13)** White powder, 72.12%; mp: 201-202°C; MS (ESI): *m/z* 305.2 $(M+H)^+$; HRMS (ESI): *m/z* 671.17073 calcd 671.18869 for $C_{32}H_{40}CuN_4O_4S_2$ $(2M+Cu)^+$; ^{1}H-NMR (δ): (400 MHz, $CDCl_3$) δ 11.45 (s, 1H), 7.65 (d, *J* = 8.8 Hz, 1H), 7.27 (d, *J* = 2.5 Hz, 1H), 7.00 (dd, *J* = 8.8, 2.5 Hz, 1H), 3.87 (s, 3H), 1.33 (s, 6H), 1.11 (s, 1H), 1.06 (s, 6H); ^{13}C-NMR (δ): (101 MHz, $CDCl_3$) δ 170.49, 158.12, 156.64, 141.97, 132.98, 121.03, 114.92, 104.37, 55.87, 37.48, 23.53, 16.59.

3.1.3 Procedure for the synthesis of [*N*-(3-Substituted)-4-/6-methoxy/unsubstituted-3*H*-benzothiazol-2-ylidene]-carboxamide derivatives (14-33)

To a solution of the appropriate *N*-(benzothiazol-2-yl) carboxamide (1.28 mmol) in dry DMF (4.0 mL), NaH was added (60% in mineral oil, 1.92 mmol), the mixture was stirred for 1 hour at room temperature. Thereafter the appropriate alkyl bromide (1.41 mmol) was added, and the reaction mixture was heated at 80°C for 24 hours. Afterwards, the mixture was cooled to room temperature, quenched with iced water and extracted with ethyl acetate. The organic layer was dried over anhydrous $MgSO_4$, filtered, and then evaporated. The resulting residue was further purified using column chromatography.

***N*-[3-(2-Methoxyethyl)-3*H*-benzothiazol-2-ylidene]-3-trifluoromethyl-benzamide (14)** White crystals, 61.97%; mp: 115-117°C; MS (ESI): *m/z* 381.2 $(M+H)^+$; HRMS (ESI): *m/z* 403.0699 calcd 403.0704 for $C_{18}H_{15}F_3N_2NaO_2S$ $(M+Na)^+$; ^{1}H-NMR (δ): (300 MHz, $CDCl_3$) δ 8.62 (s, 1H), 8.52 (d, *J* = 7.8 Hz, 1H), 7.77 (d, *J* = 7.8 Hz, 1H), 7.70 (d, *J* = 7.5 Hz, 1H), 7.63 – 7.51 (m, 2H), 7.51 – 7.43 (m, 1H), 7.36 – 7.28 (m, 1H), 4.71 (t, *J* = 5.6 Hz, 2H), 3.91 (t, *J* = 5.6 Hz, 2H), 3.36 (s, 3H); ^{13}C-NMR (δ): (75 MHz, $CDCl_3$) δ 173.44, 167.96, 137.40, 137.26, 132.58, 130.58 (q, $^2J_{CF}$ = 32.5 Hz), 128.67, 128.24 (q, $^3J_{CF}$ = 3.5 Hz), 126.99, 126.48, 126.34 (q, $^3J_{CF}$ = 3.9 Hz), 124.08 (q, $^1J_{CF}$ = 270.8 Hz), 124.00, 122.72, 112.45, 69.72, 59.12, 45.95.

***N*-[3-(4-Fluorobutyl)-3*H*-benzothiazol-2-ylidene]-3-trifluoromethyl-benzamide (15)** White powder, 81.07%; mp: 118-119°C; MS (ESI): *m/z* 397.2 $(M+H)^+$; HRMS (ESI): *m/z* 419.0812 calcd 419.0817 for $C_{19}H_{16}F_4N_2NaOS$ $(M+Na)^+$; ^{1}H-NMR (δ): (300 MHz, $CDCl_3$) δ 8.65 (s, 1H), 8.52 (d, *J* = 7.8 Hz, 1H), 7.81 – 7.71 (m, 2H), 7.60 (t, *J* = 7.7 Hz, 1H), 7.54 – 7.46 (m, 1H), 7.44 – 7.30 (m, 2H), 4.69 – 4.57 (m, 3H), 4.48 (t, *J* = 5.7 Hz, 1H), 2.20 – 2.02 (m, 2H), 1.99 – 1.77 (m, 2H); ^{13}C-NMR (δ): (75 MHz, $CDCl_3$) δ 173.50, 167.89, 137.40, 136.44, 132.53, 130.61 (d, $^2J_{CF}$ = 32.6 Hz), 128.71, 128.26 (q, $^3J_{CF}$ = 4.1 Hz), 127.15, 126.88, 126.37 (q, $^3J_{CF}$ = 3.8 Hz), 124.09, 123.13, 122.27, 111.51, 83.44 (d, $^1J_{CF}$ = 165.8 Hz), 45.39, 27.73 (d, $^2J_{CF}$ = 20.0 Hz), 24.01 (d, $^3J_{CF}$ = 4.1 Hz).

***N*-[4-Methoxy-3-(2-methoxyethyl)-3*H*-benzothiazol-2-ylidene]-3-trifluoromethyl-benzamide (16)** White powder, 64.64%; mp: 131-133°C; MS (ESI): *m/z* 411.2 $(M+H)^+$; HRMS (ESI): *m/z* 411.09958 calcd 411.09902 for $C_{19}H_{18}F_3N_2O_3S$ $(M+H)^+$; ^{1}H-NMR (δ): (400 MHz, $CDCl_3$) δ 8.68 (s, 1H), 8.56 (d, *J* = 7.8 Hz, 1H), 7.79 (d, *J* = 7.7 Hz, 1H), 7.62 (t, *J* = 7.8 Hz, 1H), 7.33 (dd, *J* = 7.9, 1.2 Hz, 1H), 7.29 (t, *J* = 3.9 Hz, 1H), 7.00 (dd, *J* = 7.9, 1.1 Hz, 1H), 5.15 (t, *J* = 6.6 Hz, 2H), 4.03 (s, 3H), 3.88 (t, *J* = 6.6 Hz, 2H), 3.47 (s, 3H); ^{13}C-NMR (δ): (101 MHz,

$CDCl_3$) δ 173.45, 168.16, 147.48, 137.61, 132.59, 130.57 (q, $^2J_{CF}$ = 32.5 Hz), 128.67, 128.57, 128.14 (q, $^3J_{CF}$ = 3.4 Hz), 126.37 (q, $^3J_{CF}$ = 3.8 Hz), 125.91, 124.13 (q, $^1J_{CF}$ = 266.3), 124.70, 115.25, 109.60, 70.28, 59.00, 56.15, 47.33.

***N*-[3-(4-Fluorobutyl)-4-methoxy-3*H*-benzothiazol-2-ylidene]-3-trifluoromethyl-benzamide (17)** Yellow powder, 68.19%; mp: 133-134°C; MS (ESI): *m/z* 427.2 $(M+H)^+$; HRMS (ESI): *m/z* 449.09363 calcd 449.09228 for $C_{20}H_{18}F_4N_2NaO_2S$ $(M+Na)^+$; ^{1}H-NMR (δ): (400 MHz, $CDCl_3$) δ 8.67 (s, 1H), 8.54 (d, *J* = 7.8 Hz, 1H), 7.78 (d, *J* = 7.7 Hz, 1H), 7.62 (t, *J* = 7.8 Hz, 1H), 7.33 (dd, *J* = 7.9, 1.2 Hz, 1H), 7.28 (t, *J* = 7.9 Hz, 1H), 6.99 (dd, *J* = 8.0, 1.0 Hz, 1H), 4.98 (t, *J* = 6.0 Hz, 2H), 4.57 (dt, *J* = 47.3, 5.8 Hz, 2H), 4.02 (s, 3H), 2.13 - 2.06 (m, 2H), 1.97 – 1.83 (m, 2H); ^{13}C-NMR (δ): (101 MHz, $CDCl_3$) δ 173.38, 167.74, 147.43, 137.67, 132.51, 130.57 (q, $^2J_{CF}$ = 32.5 Hz), 128.71, 128.68, 128.11 (q, $^3J_{CF}$ = 3.4 Hz), 126.35 (q, $^3J_{CF}$ = 3.7 Hz), 125.80, 124.14 (q, $^1J_{CF}$ = 273.04 Hz), 124.69, 115.24, 109.41, 83.57 (d, $^1J_{CF}$ = 165.5 Hz), 56.05, 48.41, 27.79 (d, $^2J_{CF}$ = 20.1 Hz), 25.73 (d, $^3J_{CF}$ = 4.4 Hz).

***N*-[6-Methoxy-3-(2-methoxyethyl)-3*H*-benzothiazol-2-ylidene]-3-trifluoromethyl-benzamide (18)** White powder, 68.70%; mp: 166-167°C; MS (ESI): *m/z* 411.2 $(M+H)^+$; HRMS (ESI): *m/z* 433.08184 calcd 433.08096 for $C_{19}H_{17}F_3N_2NaO_3S$ $(M+Na)^+$; ^{1}H-NMR (δ): (400 MHz, $CDCl_3$) δ 8.61 (t, *J* = 1.7 Hz, 1H), 8.54 – 8.47 (m, 1H), 7.78 – 7.74 (m, 1H), 7.58 (td, *J* = 7.8, 0.6 Hz, 1H), 7.44 (d, *J* = 9.0 Hz, 1H), 7.20 (d, *J* = 2.5 Hz, 1H), 7.05 (dd, *J* = 9.0, 2.5 Hz, 1H), 4.67 (t, *J* = 5.6 Hz, 2H), 3.89 (t, *J* = 5.7 Hz, 2H), 3.87 (s, 3H), 3.35 (s, 3H); ^{13}C-NMR (δ): (101 MHz, $CDCl_3$) δ 173.17, 167.32, 156.85, 137.51, 132.52, 131.20, 130.54 (q, $^2J_{CF}$ = 32.4 Hz), 128.62, 128.11 (q, $^3J_{CF}$ = 3.7 Hz), 127.77, 126.28 (q, $^3J_{CF}$ = 3.9 Hz), 124.09(q, $^1J_{CF}$ = 292.9), 115.03, 113.27, 106.31, 69.82, 59.13, 55.92, 46.11.

***N*-[3-(4-Fluorobutyl)-6-methoxy-3*H*-benzothiazol-2-ylidene]-3-trifluoromethyl-benzamide (19)** Yellow powder**,** 66.12%; mp: 124-126°C; MS (ESI): *m/z* 427.2 $(M+H)^+$; HRMS (ESI): *m/z* 875.19144 calcd 875.19479 for $C_{40}H_{36}F_8N_4NaO_4S_2$ $(2M+Na)^+$; ^{1}H-NMR (δ): (400 MHz, $CDCl_3$) δ 8.63 (s, 1H), 8.52 (d, *J* = 7.8 Hz, 1H), 7.77 (d, *J* = 7.7 Hz, 1H), 7.60 (t, *J* = 7.8 Hz, 1H), 7.32 (d, *J* = 8.9 Hz, 1H), 7.24 (d, *J* = 2.4 Hz, 1H), 7.07 (dd, *J* = 8.9, 2.5 Hz, 1H), 4.65 – 4.57 (m, 3H), 4.49 (t, *J* = 5.7 Hz, 1H), 3.88 (s, 3H), 2.14 – 2.04 (m, 2H), 1.95 – 1.80 (m, 2H); ^{13}C-NMR (δ): (101 MHz, $CDCl_3$) δ 173.08, 167.11, 157.02, 137.29, 132.55, 130.61 (q, $^2J_{CF}$ = 32.6 Hz), 130.32, 128.70, 128.25, 126.38 (q, $^3J_{CF}$ = 3.7 Hz), 124.10 (q, $^1J_{CF}$ = 288.5 Hz), 115.30, 112.39, 106.78, 83.45 (d, $^1J_{CF}$ = 165.6 Hz), 55.99, 45.64, 27.70 (d, $^2J_{CF}$ = 20.1 Hz), 24.10 (d, $^3J_{CF}$ = 4.1 Hz).

***N*-[3-(2-Methoxyethyl)-3*H*-benzothiazol-2-ylidene]-1-adamantyl-carboxamide (20)** Yellow powder, 83.23%; mp: 151-153°C; MS (ESI): *m/z* 371.2 $(M+H)^+$; HRMS (ESI): *m/z* 393.1607 calcd 393.1613 for $C_{21}H_{26}N_2NaO_2S$ $(M+Na)^+$; ^{1}H-NMR (δ): (300 MHz, $CDCl_3$) δ 7.62 (d, *J* = 7.7 Hz, 1H), 7.45 – 7.36 (m, 2H), 7.25 – 7.20 (m, 1H), 4.54 (t, *J* = 5.7 Hz, 2H), 3.81 (t, *J* = 5.7 Hz, 2H), 3.33 (s, 3H), 2.05 (s, 3H), 1.99 (d, *J* = 2.6 Hz, 6H), 1.75 (s, 6H); ^{13}C-NMR (δ): (75 MHz, $CDCl_3$) δ 188.59, 166.94, 137.25, 126.59, 126.55, 123.30, 122.57, 111.81, 69.64, 59.11, 45.53, 42.94, 39.40, 36.89, 28.40.

***N*-[3-(4-Fluorobutyl)-3*H*-benzothiazol-2-ylidene]-1-adamantyl-carboxamide (21)** Yellow powder, 64.68%; mp: 131-132°C; MS (ESI): *m/z* 387.2 $(M+H)^+$; HRMS (ESI): *m/z* 409.1720 calcd 409.1726 for $C_{22}H_{27}FN_2NaOS$ $(M+Na)^+$; ^{1}H-NMR (δ): (300 MHz, $CDCl_3$) δ 7.65 (d, *J* = 7.8 Hz, 1H), 7.45 – 7.39 (m, 1H), 7.33 – 7.22 (m, 2H), 4.60 (t, *J* = 5.7 Hz, 1H), 4.50 – 4.41 (m, 3H), 2.06 (s, 3H), 2.03 – 1.95 (m, 8H), 1.87 – 1.79 (m, 2H), 1.76 (s, 6H); ^{13}C-NMR (δ): (75

MHz, $CDCl_3$) δ 188.67, 167.04, 136.48, 126.98, 126.68, 123.39, 122.93, 110.97, 83.51 (d, $^1J_{CF}$ = 165.3 Hz), 44.88, 42.94, 39.40, 36.89, 28.39, 27.67 (d, $^2J_{CF}$ = 20.1 Hz), 23.72 (d, $^3J_{CF}$ = 4.6 Hz).

***N*-[4-Methoxy-3-(2-methoxyethyl)-3*H*-benzothiazol-2-ylidene]-1-adamantyl-carboxamide**

(22) White crystals, 60.34%; mp: 185-186°C; MS (ESI): *m/z* 401.3 $(M+H)^+$; HRMS (ESI): *m/z* 401.19120 calcd 401.18989 for $C_{22}H_{29}N_2O_3S$ $(M+H)^+$; ^{1}H-NMR (δ): (400 MHz, $CDCl_3$) δ 7.22 (dd, *J* = 7.8, 1.3 Hz, 1H), 7.17 (t, *J* = 7.9 Hz, 1H), 6.91 (dd, *J* = 7.9, 1.2 Hz, 1H), 4.97 (t, *J* = 6.8 Hz, 2H), 3.96 (s, 3H), 3.77 (t, *J* = 6.8 Hz, 2H), 3.42 (s, 3H), 2.05 (s, 3H), 2.00 (d, *J* = 2.9 Hz, 6H), 1.75 (t, *J* = 2.9 Hz, 6H); ^{13}C-NMR (δ): (101 MHz, $CDCl_3$) δ 188.57, 167.24, 147.12, 128.61, 125.83, 123.93, 115.18, 109.35, 70.03, 58.97, 56.06, 46.81, 42.91, 39.42, 36.91, 28.42.

***N*-[3-(4-Fluorobutyl)-4-methoxy-3*H*-benzothiazol-2-ylidene]-1-adamantyl-carboxamide**

(23) White powder**,** 59.79%; mp: 149-151°C; MS (ESI): *m/z* 417.3 $(M+H)^+$; HRMS (ESI): *m/z* 417.20267 calcd 417.20120 for $C_{23}H_{30}FN_2O_2S$ $(M+H)^+$; ^{1}H-NMR (δ): (400 MHz, $CDCl_3$) δ 7.24 (dd, *J* = 7.8, 1.3 Hz, 1H), 7.19 (t, *J* = 7.9 Hz, 1H), 6.92 (dd, *J* = 7.9, 1.2 Hz, 1H), 4.86 (t, *J* = 8.0 Hz, 2H), 4.51 (dt, *J* = 47.4, 5.9 Hz, 2H), 3.96 (s, 3H), 2.06 (s, 3H), 2.01 (d, *J* = 2.7 Hz, 6H), 1.98 – 1.93 (m, 2H), 1.88 – 1.78 (m, 2H), 1.76 (d, *J* = 2.9 Hz, 6H); ^{13}C-NMR (δ): (101 MHz, $CDCl_3$) δ 188.09, 166.82, 147.20, 128.80, 125.72, 124.19, 115.16, 109.26, 83.67 (d, $^1J_{CF}$ = 165.2 Hz), 56.00, 48.16, 42.93, 39.37, 36.89, 28.43, 27.70 (d, $^2J_{CF}$ = 20.0 Hz), 25.48 (d, $^3J_{CF}$ = 4.7 Hz).

***N*-[6-Methoxy-3-(2-methoxyethyl)-3*H*-benzothiazol-2-ylidene]-1-adamantyl-carboxamide**

(24) White powder, 80.95%; mp: 144-146°C; MS (ESI): *m/z* 401.17 $(M+H)^+$; ^{1}H-NMR (δ): (400 MHz, $CDCl_3$) δ 7.33 (d, *J* = 8.9 Hz, 1H), 7.14 (d, *J* = 2.5 Hz, 1H), 6.98 (dd, *J* = 8.9, 2.5 Hz, 1H),

4.50 (t, *J* = 5.6 Hz, 2H), 3.84 (s, 3H), 3.79 (t, *J* = 5.6 Hz, 2H), 3.33 (s, 3H), 2.05 (s, 3H), 1.99 (d, *J* = 2.8 Hz, 6H), 1.75 (s, 6H); ^{13}C-NMR (δ): (101 MHz, $CDCl_3$) δ 188.36, 166.50, 156.37, 131.24, 127.86, 114.41, 112.59, 106.47, 69.75, 59.14, 55.91, 45.73, 42.85, 39.48, 36.93, 28.45.

***N*-[3-(4-Fluorobutyl)-6-methoxy-3*H*-benzothiazol-2-ylidene]-1-adamantyl-carboxamide (25)** Yellow powder, 75.48%; mp: 114-115°C; MS (ESI): *m/z* 417.3 $(M+H)^+$; HRMS (ESI): *m/z* 855.37686 calcd 855.37652 for $C_{46}H_{58}F_2N_4NaO_4S_2$ $(2M+Na)^+$; ^{1}H-NMR (δ): (400 MHz, $CDCl_3$) δ 7.20 (d, *J* = 8.9 Hz, 1H), 7.17 (d, *J* = 2.5 Hz, 1H), 6.99 (dd, *J* = 8.9, 2.5 Hz, 1H), 4.57 (t, *J* = 5.8 Hz, 1H), 4.44 (dt, J = 9.7, 6.5 Hz, 3H), 3.85 (s, 3H), 2.05 (s, 3H), 2.01 – 1.94 (m, 8H), 1.86 – 1.77 (m, 2H), 1.75 (s, 6H); ^{13}C-NMR (δ): (101 MHz, $CDCl_3$) δ 188.46, 166.61, 156.44, 130.39, 128.31, 114.51, 111.70, 106.90, 83.54 (d, $^1J_{CF}$ = 165.4 Hz), 55.94, 44.99, 42.86, 39.47, 36.93, 28.44, 27.66 (d, $^2J_{CF}$ = 20.1 Hz), 23.77 (d, $^3J_{CF}$ = 4.4 Hz).

***N*-[3-(2-Methoxyethyl)-3*H*-benzothiazol-2-ylidene]-1-naphthyl-carboxamide (26)** Yellow powder, 80.40%; mp: 78-79°C; MS (ESI): *m/z* 363.2 $(M+H)^+$; HRMS (ESI): *m/z* 385.0981 calcd 385.0987 for $C_{21}H_{18}N_2NaO_2S$ $(M+Na)^+$; ^{1}H-NMR (δ): (300 MHz, $CDCl_3$) δ 9.27 (d, *J* = 8.4 Hz, 1H), 8.51 (dd, *J* = 7.3, 1.2 Hz, 1H), 7.99 (d, *J* = 8.2 Hz, 1H), 7.89 (d, *J* = 7.5 Hz, 1H), 7.74 – 7.69 (m, 1H), 7.65 – 7.42 (m, 5H), 7.36 – 7.28 (m, 1H), 4.69 (t, *J* = 5.6 Hz, 2H), 3.90 (t, *J* = 5.6 Hz, 2H), 3.35 (s, 3H); ^{13}C-NMR (δ): (75 MHz, $CDCl_3$) δ 177.04, 167.05, 140.02, 137.33, 134.00, 132.20, 131.72, 130.01, 128.32, 127.03, 126.82, 126.59, 125.80, 124.63, 123.72, 122.68, 112.20, 69.96, 59.16, 45.92.

***N*-[3-(4-Fluorobutyl)-3*H*-benzothiazol-2-ylidene]-1-naphthyl- carboxamide (27)** Yellow powder, 72.06%; mp: 93-94°C; MS (ESI): *m/z* 379.2 $(M+H)^+$; HRMS (ESI): *m/z* 401.1094 calcd 401.1100 for $C_{22}H_{19}FN_2NaOS$ $(M+Na)^+$; ^{1}H-NMR (δ): (400 MHz, $CDCl_3$) δ 9.29 (d, *J* = 8.1 Hz,

1H), 8.53 (dd, *J* = 7.3, 1.3 Hz, 1H), 8.00 (d, *J* = 8.1 Hz, 1H), 7.90 (d, *J* = 8.0 Hz, 1H), 7.74 (d, *J* = 7.7 Hz, 1H), 7.65 – 7.44 (m, 4H), 7.43 – 7.29 (m, 2H), 4.66 – 4.55 (m, 3H), 4.45 (t, *J* = 5.7 Hz, 1H), 2.18 – 2.01 (m, 2H), 1.95 – 1.79 (m, 2H); ^{13}C-NMR (δ): (75 MHz, $CDCl_3$) δ 177.10, 166.99, 136.52, 134.02, 133.88, 132.23, 131.73, 130.02, 128.34, 127.03, 126.98, 126.97, 126.80, 125.81, 124.67, 123.80, 123.06, 111.26, 83.49 (d, $^1J_{CF}$ = 165.6 Hz), 45.27, 27.74 (d, $^2J_{CF}$ = 20.1 Hz), 23.99 (d, $^3J_{CF}$ = 4.3 Hz).

***N*-[3-(2-Methoxyethyl)-3*H*-benzothiazol-2-ylidene]-2,2,3,3-tetramethyl-cyclopropyl-carboxamide (28)** White powder, 65.26%; mp: 109-111°C; MS (ESI): *m/z* 333.2 $(M+H)^+$; HRMS (ESI): *m/z* 355.1451 calcd 355.1456 for $C_{18}H_{24}N_2NaO_2S$ $(M+Na)^+$; ^{1}H-NMR (δ): (300 MHz, $CDCl_3$) δ 7.57 (d, *J* = 7.8 Hz, 1H), 7.44 – 7.35 (m, 2H), 7.25 – 7.19 (m, 1H), 4.52 (t, *J* = 5.7 Hz, 2H), 3.79 (t, *J* = 5.7 Hz, 2H), 3.34 (s, 3H), 1.65 (s, 1H), 1.36 (s, 6H), 1.24 (s, 6H); ^{13}C-NMR (δ): (75 MHz, $CDCl_3$) δ 182.86, 164.24, 137.13, 126.44, 126.40, 123.19, 122.42, 111.73, 69.79, 45.33, 31.50, 29.68, 24.03, 16.88.

***N*-[3-(4-Fluorobutyl)-3*H*-benzothiazol-2-ylidene]-2,2,3,3-tetramethyl-cyclopropyl-carboxamide (29)** Yellow powder, 66.25%; mp: 128-130°C; MS (ESI): *m/z* 349.2 $(M+H)^+$; HRMS (ESI): *m/z* 371.1564 calcd 371.1569 for $C_{19}H_{25}FN_2NaOS$ $(M+Na)^+$; ^{1}H-NMR (δ): (300 MHz, $CDCl_3$) δ 7.60 (d, *J* = 7.7 Hz, 1H), 7.44 – 7.37 (m, 1H), 7.26 (t, *J* = 7.1 Hz, 2H), 4.62 (t, *J* = 5.7 Hz, 1H), 4.50 – 4.39 (m, 3H), 2.04 – 1.92 (m, 2H), 1.91 – 1.72 (m, 2H), 1.64 (s, 1H), 1.36 (s, 6H), 1.25 (s, 6H); ^{13}C-NMR (δ): (75 MHz, $CDCl_3$) δ 182.90, 164.20, 136.38, 126.82, 126.59, 123.26, 122.78, 110.86, 83.47 (d, $^1J_{CF}$ = 165.2 Hz), 44.62, 42.84, 27.55 (d, $^2J_{CF}$ = 20.1 Hz), 24.03, 23.57 (d, $^3J_{CF}$ = 4.5 Hz), 16.90.

***N*-[4-Methoxy-3-(2-methoxyethyl)-3*H*-benzothiazol-2-ylidene]-2,2,3,3-tetramethyl-cyclopropyl-carboxamide (30)** White powder**,** 72.38%; mp: 128-130°C; MS (ESI): *m/z* 363.2

$(M+H)^+$; HRMS (ESI): *m/z* 385.15643 calcd 385.15618 for $C_{19}H_{26}N_2NaO_3S$ $(M+Na)^+$; ^{1}H-NMR (δ): (400 MHz, $CDCl_3$) δ 7.19 – 7.12 (m, 2H), 6.89 (dd, *J* = 7.2, 2.0 Hz, 1H), 4.93 (t, *J* = 6.7 Hz, 2H), 3.95 (s, 3H), 3.75 (t, *J* = 6.7 Hz, 2H), 3.42 (s, 3H), 1.66 (s, 1H), 1.36 (s, 6H), 1.23 (s, 6H); ^{13}C-NMR (δ): (101 MHz, $CDCl_3$) δ 182.84, 164.59, 147.01, 128.47, 125.64, 123.83, 115.08, 109.28, 70.24, 58.88, 56.01, 46.64, 42.84, 24.02, 16.91.

***N*-[3-(4-Fluorobutyl)-4-methoxy-3*H*-benzothiazol-2-ylidene]-2,2,3,3-tetramethyl-cyclopropyl-carboxamide (31)** White crystals**,** 61.30%; mp: 154-155°C; MS (ESI): *m/z* 379.2 $(M+H)^+$; HRMS (ESI): *m/z* 779.34852 calcd 779.34522 for $C_{40}H_{54}F_2N_4NaO_4S_2$ $(2M+Na)^+$; ^{1}H-NMR (δ): (400 MHz, $CDCl_3$) δ 7.21 – 7.12 (m, 2H), 6.89 (dd, *J* = 7.4, 1.8 Hz, 1H), 4.75 (t , *J* = 8.0 Hz, 2H), 4.53 (dt, *J* = 47.4, 6.0 Hz, 2H), 3.95 (s, 3H), 1.98 – 1.91 (m, 2H), 1.87 – 1.72 (m, 2H), 1.63 (s, 1H), 1.36 (s, 6H), 1.24 (s, 6H); ^{13}C-NMR (δ): (101 MHz, $CDCl_3$) δ 182.85, 164.41, 147.01, 128.64, 125.58, 123.86, 115.08, 109.13, 83.66 (d, $^1J_{CF}$ = 164.9 Hz), 55.94, 47.56, 42.86, 27.60 (d, $^2J_{CF}$ = 20.0 Hz), 25.40 (d, $^3J_{CF}$ = 4.8 Hz), 24.07, 16.95.

***N*-[6-Methoxy-3-(2-methoxyethyl)-3*H*-benzothiazol-2-ylidene]-2,2,3,3-tetramethyl-cyclopropyl-carboxamide (32)** Yellow powder, 68.19%; mp: 88-90°C; MS (ESI): *m/z* 363.2 $(M+H)^+$; HRMS (ESI): *m/z* 385.15729 calcd 385.15618 for $C_{19}H_{26}N_2NaO_3S$ $(M+Na)^+$; ^{1}H-NMR (δ): (300 MHz, $CDCl_3$) δ 7.31 (d, *J* = 8.9 Hz, 1H), 7.08 (d, *J* = 2.5 Hz, 1H), 6.96 (dd, *J* = 8.9, 2.6 Hz, 1H), 4.48 (t, *J* = 5.7 Hz, 2H), 3.83 (s, 3H), 3.77 (t, *J* = 5.7 Hz, 2H), 3.32 (s, 3H), 1.62 (s, 1H), 1.35 (s, 6H), 1.23 (s, 6H); ^{13}C-NMR (δ): (75 MHz, $CDCl_3$) δ 182.63, 163.87, 156.29, 131.08, 127.67, 114.07, 112.48, 106.48, 69.90, 59.06, 55.89, 45.51, 42.72, 24.03, 16.90.

***N*-[3-(4-Fluorobutyl)-6-methoxy-3*H*-benzothiazol-2-ylidene]-2,2,3,3-tetramethyl-cyclopropyl-carboxamide (33)** White powder, 80.95%; mp: 87-88°C; MS (ESI): *m/z* 379.2 $(M+H)^+$; HRMS (ESI): *m/z* 401.17064 calcd 401.16749 for $C_{20}H_{27}FN_2NaO_2S$ $(M+Na)^+$; ^{1}H-NMR (δ): (400 MHz, DMSO) δ 7.55 (d, *J* = 9.0 Hz, 1H), 7.44 (d, *J* = 2.5 Hz, 1H), 7.07 (dd, *J* = 8.9, 2.6 Hz, 1H), 4.55 (t, *J* = 5.8 Hz, 2H), 4.40 (dt, *J* = 14.2, 6.6 Hz, 2H), 3.80 (s, 3H), 1.87 – 1.75 (m, 2H), 1.73 – 1.64 (m, 2H), 1.57 (s, 1H), 1.27 (s, 6H), 1.19 (s, 6H); ^{13}C-NMR (δ): (101 MHz, DMSO) δ 181.52, 163.60, 156.54, 130.41, 127.46, 114.91, 113.23, 107.52, 83.87 (d, $^1J_{CF}$ = 161.8 Hz), 56.22, 44.93, 42.31, 27.51 (d, $^2J_{CF}$ = 19.6 Hz), 24.22, 23.58 (d, $^3J_{CF}$ = 5.2 Hz), 17.18.

3.1.4. Procedure for the synthesis of *N*-[3-(2-Hydroxyethyl)-4-methoxy/unsubstituted-3*H*-benzothiazol-2-ylidene]-2,2,3,3-tetramethyl-cyclopropyl-carboxamide derivatives (36, 37)

2-Aminobenzothiazole (1 mmol) and 2-bromoethan-1-ol (1.5 mmol) were reacted in a sealed vessel at 90°C for 16-24 hours. The resulting residue was dried under high vacuum and used in the next step without further purification.

2, 2, 3, 3-Tetramethylcyclopropane carboxylic acid (1 mmol), TEA (3 mmol) and BOP (1.3 mmol) were added to a suspension of the 3-alkylated-2-aminobenzothiazole (1 mmol) in 5 mL DCM at 0 °C, and the mixture was stirred at room temperature for 24 hours. The reaction was quenched by addition of 2 mL water followed by a 10 mL aqueous saturated solution of $NaHCO_3$ and 15 mL ethyl acetate. The phases were separated and the aqueous phase was washed with 2x10 mL ethyl acetate. The combined organic fractions were washed with 20 mL brine, dried over $MgSO_4$ and concentrated by rotary evaporation. The obtained residue was purified by column chromatography.

***N*-[3-(2-Hydroxyethyl)-3*H*-benzothiazol-2-ylidene]-2,2,3,3-tetramethyl-cyclopropyl-carboxamide (36)** Yellowish white crystals, 78.01%; mp: 121-122°C; MS (ESI): *m/z* 319.2 $(M+H)^+$; HRMS (ESI): *m/z* 341.13272 calcd 341.12996 for $C_{17}H_{22}N_2NaO_2S$ $(M+Na)^+$; ^{1}H-NMR (δ): (400 MHz, $CDCl_3$) δ 7.60 (d, *J* = 7.2 Hz, 1H), 7.44 – 7.38 (m, 1H), 7.32 – 7.23 (m, 2H), 4.53(t, *J* = 6.0 Hz, 2H), 4.08 (t, *J* = 6.0 Hz, 2H), 1.59 (s, 1H), 1.34 (s, 6H), 1.23 (s, 6H); ^{13}C-NMR (δ): (101 MHz, $CDCl_3$) δ 182.01, 166.40, 136.45, 126.86, 126.69, 123.73, 122.89, 110.99, 62.32, 48.55, 42.63, 23.93, 16.83.

***N*-[3-(2-Hydroxyethyl)-4-methoxy-3*H*-benzothiazol-2-ylidene]-2,2,3,3-tetramethyl-cyclopropyl-carboxamide (37)** White powder, 80.31%; mp: 153-155°C; MS (ESI): *m/z* 349.2 $(M+H)^+$; HRMS (ESI): *m/z* 349.16140 calcd 349.15859 for $C_{18}H_{25}N_2O_3S$ $(M+H)^+$, *m/z* 371.14255 calcd 371.14053 for $C_{18}H_{24}N_2NaO_3S$ $(M+Na)^+$; ^{1}H-NMR (δ): (400 MHz, $CDCl_3$) δ 7.22 – 7.16 (m, 2H), 6.94 – 6.88 (m, 1H), 4.98 – 4.92 (m, 3H), 4.12 – 4.09 (t, 2H), 3.94 (s, 3H), 1.58 (s, 1H), 1.33 (s, 6H), 1.23 (s, 6H); ^{13}C-NMR (δ): (101 MHz, $CDCl_3$) δ 181.84, 167.19, 147.15, 128.53, 125.56, 124.35, 115.22, 109.37, 64.14, 56.06, 51.45, 42.57, 23.92, 16.82.

3.1.5. Procedure for the synthesis of *N*-{3-[2-(2-Fluoroethoxy)-ethyl]-4-methoxy-3*H*-benzothiazol-2-ylidene}-2,2,3,3-tetramethyl-cyclopropyl-carboxamide (38)

NaH was added (60% in mineral oil, 3 mmol) to a solution of alcohol **37** (1 mmol), in 2 mL dry DMF and the mixture was stirred for 5 min at room temperature. Thereafter, the alkylating agent, 1-fluoro-2-iodoethane (5 mmol) was added, and the reaction mixture was stirred for 20-24 hours at room temperature. The reaction was quenched by addition of water (2 mL), followed by 15 mL aqueous saturated solution $NaHCO_3$ and 20 mL ethyl acetate while stirring. The phases were separated, the organic phase was washed with 20 mL ethyl acetate and the combined

organic fractions were dried over $MgSO_4$ and concentrated under reduced pressure. The resulting residue was subjected to column chromatography purification.

***N*-{3-[2-(2-Fluoroethoxy)-ethyl]-4-methoxy-3*H*-benzothiazol-2-ylidene}-2,2,3,3-tetramethyl-cyclopropyl-carboxamide (38)** Yellow powder, 65.23%; mp: 107-109°C; MS (ESI): *m/z* 271.2 $(M+H-C_8H_{13}O)^+$;^{1}H-NMR (δ): (400 MHz, $CDCl_3$) δ 7.29 (dt, *J* = 8.1, 2.7 Hz, 1H), 7.01 (dd, *J* = 8.0, 1.1 Hz, 1H), 6.83 (dd, *J* = 8.3, 1.1 Hz, 1H), 4.68 – 4.43 (m, 4H), 3.91 – 3.77 (m, 5H), 3.36 – 3.08 (m, 2H), 1.26 (s, 1H), 1.16 (s, 6H), 1.09 (s, 6H); ^{13}C-NMR (δ): (101 MHz, $CDCl_3$) δ 183.10, 156.67, 137.13, 129.68, 121.26, 110.52, 110.37, 110.07, 81.49 (d, $^1J_{CF}$ = 172.2 Hz), 66.14, 56.00, 41.87, 32.84 (d, $^2J_{CF}$ = 21.6 Hz), 30.81, 23.87, 16.52.

3.2. Biological assays

3.2.1. Competitive radioligand binding assay.

The binding affinity towards CB_1 and CB_2 receptors was determined using a protocol similar to a previously published one.[41] As follows, membrane preparations obtained from CHO cell lines stably transfected with either human CB_1 (hCB_1-CHO) or human CB_2 (hCB_2-CHO) were used in combination with [^{3}H]SR141716A (A_m = 1554 GBq/mmol; PerkinElmer LAS GmbH, Rodgau, Germany) or [^{3}H]-WIN-55,212-2 (A_m = 1480 GBq/mmol; PerkinElmer LAS GmbH, Rodgau, Germany) as specific radioligand, respectively. The incubation was performed in borosilicate glass vials in a final volume of 1 mL containing the respective cell membrane homogenate (~ 50 µg protein), the respective radioligand (~ 3 nM), and the test compounds at different concentrations (10^{-11} – 10^{-5} M) in binding buffer (50 mM TRIS-HCl, pH 7.4, 0.1% bovine serum albumin (BSA), 5 mM $MgCl_2$, 1 mM EDTA) on a shaker (300 rpm) at 21°C for 90 min. The nonspecific binding of the respective radioligand was determined by co-administration

of 10 µM CB_1/CB_2-specific CP55940. Incubations were terminated by rapid filtration through a GF-B glass fiber filter (48-Sample, Semi-Auto Harvester; Brandel, Gaithersburg, MD, USA), pre-incubated for 90 min at room temperature in a freshly prepared solution of polyvinylpyrrolidone/Tween 20 (0.5%/0.1%). Filter-bound radioactivity was measured by liquid scintillation counting (Hodex 600 SL; Hidex, Turku, Finalnd), IC_{50} values estimated from the experimentally determined values by nonlinear regression (Prism 3.0; GraphPad Software, San Diego, CA, USA), and K_i values were estimated by the Cheng-Prusoff equation implemented in the software using a K_D value for [^{3}H]-WIN-55,212-2 is 3.3 nM and K_D value for [^{3}H]SR141716A is 2.3 nM .

3.2.2. In vitro metabolic studies

For microsome experiments, the following instruments were used BioShake iQ (QUANTIFOIL Instruments, Jena, Germany), Centrifuge 5424 (Eppendorf, Hamburg, Germany), DB-3DTECHNE Sample Concentrator (Biostep, Jahnsdorf, Germany), UltiMate 3000 UHPLC System (Thermo Scientific, Germering, Germany) including a DAD detector (DAD-3000RS) coupled to an MSQ Plus Single Quadrupole Mass Spectrometer (Thermo Scientific, Austin, Texas, USA).

Incubations had a final volume of 250 µL and were performed in PBS (pH 7.4) following a described method.[42] **21** and **29** were freshly dissolved in DMSO to provide a stock solution of 50 µM for each that was used for the experiments and resulted in an amount of DMSO of ≤0.35% in each incubation mixture (final concentrations stated in brackets). PBS, MLM or HLM (1 mg/mL each), and **21** or **29** (20 µM each) were mixed and preincubated at 3 °C for 5 min. Analogously preincubated NADPH (2 mM) was added, and the mixtures were gently shaken at 37 °C. After defined timepoints (30 min / 60 min; for testosterone 90 min), 1.0 mL of cold

acetonitrile (−20°C) was added, followed by vigorous shaking (30 s), cooling on ice (4 min), and centrifugation at 14,000 rpm (10 min). Supernatants were concentrated at 50 °C under a flow of nitrogen to provide residual volumes of 40–60 µL, which were reconditioned by addition of water to obtain samples of 100 µL, which were stored at 4 °C until analyzed by HPLC-UV-MS. Incubations at different time points in MLM/HLM were done in duplicate, to ensure reproducibility. As a positive control for proving the assay, testosterone was used as substrate and incubated at an appropriate concentration, similar to the protocol described above, to give complete conversion, as confirmed by HPLC. Furthermore, incubations without NADPH, microsomal protein, and **21** or **29**, respectively, were performed in the same manner, as negative controls.

For HPLC-UV-MS analyses chromatographic separation was performed using a ReproSil-Pur Basic C18-HD-column, 150 mm×3 mm, 3 µm (Dr. Maisch GmbH, Ammerbuch, Germany) equipped with an appropriate precolumn. The solvent system consisted of Eluent A: acetonitrile/ ammonium acetate (20 mM) in water 10/90 (*v*:*v*), and Eluent B: acetonitrile/ ammonium acetate (20 mM) in water 90/10 (*v*:*v*). Elution was performed as gradient as follows (% of eluent B): 0–1 min, 0%; 1-10 min, 0-100%; 10-18.5 min, 100%; 18.5-25min, 0%, at a flow rate of 0.6 mL/min and a column temperature of 25°C. UV detection was performed at a wavelength of 320 nm (maximum UV absorbance of compounds under investigation) and a bandwidth of 20 nm. The MSQ Plus single quadrupole mass spectrometer was operated in positive electrospray ionization mode: probe temperature 575 °C, needle voltage 4 V, and cone voltage 75 V.

Fractions of residual substrate (**21** or **29**) after 30 min of 60 min, respectively, were calculated from the peak areas (UV detection) for substrate (A_S) and the sum of peak areas of formed metabolites (ΣA_M) as follows: Fraction (%) = A_S x 100% / (A_S + ΣA_M)

4. References

1. Han, S., Thatte, J., Buzard, D. J. & Jones, R. M. Therapeutic utility of cannabinoid receptor type 2 (CB2) selective agonists. *J. Med. Chem.* **56**, 8224–8256 (2013).

2. Hampson, R. E. & Deadwyler, S. A. Cannabinoids, hippocampal function and memory. *Life Sci.* **65**, 715–723 (1999).

3. Beltramo, M. & Piomelli, D. Trick or treat from food endocannabinoids? *Nature* **396**, 636–637 (1998).

4. Bellocchio, L., Cervino, C., Pasquali, R. & Pagotto, U. The endocannabinoid system and energy metabolism. *J. Neuroendocrinol.* **20**, 850–857 (2008).

5. Pandey, R., Mousawy, K., Nagarkatti, M. & Nagarkatti, P. Endocannabinoids and immune regulation. *Pharmacol. Res.* **60**, 85–92 (2009).

6. Donvito, G. *et al.* The Endogenous Cannabinoid System: A Budding Source of Targets for Treating Inflammatory and Neuropathic Pain. *Neuropsychopharmacology* **43**, 52–79 (2018).

7. Aizpurua-Olaizola, O. *et al.* Targeting the endocannabinoid system: future therapeutic strategies. *Drug Discov. Today* **22**, 105–110 (2017).

8. Matsuda, L. A., Lolait, S. J., Brownstein, M. J., Young, A. C. & Bonner, T. I. Structure of a cannabinoid receptor and functional expression of the cloned cDNA. *Nature* **346**, 561–564 (1990).

9. Munro, S., Thomas, K. L. & Abu-Shaar, M. Molecular characterization of a peripheral receptor for cannabinoids. *Nature* **365**, 61–65 (1993).

10. Reggio, P. Endocannabinoid Binding to the Cannabinoid Receptors: What Is Known and What Remains Unknown. *Curr. Med. Chem.* **17**, 1468–1486 (2010).

11. Murataeva, N., Straiker, A. & MacKie, K. Parsing the players: 2-arachidonoylglycerol synthesis and degradation in the CNS. *Br. J. Pharmacol.* **171**, 1379–1391 (2014).

12. Piomelli, D. The molecular logic of endocannabinoid signalling. *Nat. Rev. Neurosci.* **4**, 873–884 (2003).

13. Van Sickle, M. D. *et al.* Neuroscience: Identification and functional characterization of brainstem cannabinoid CB2 receptors. *Science (80-.).* **310**, 329–332 (2005).

14. Brusco, A., Tagliaferro, P., Saez, T. & Onaivi, E. S. Postsynaptic localization of CB2 cannabinoid receptors in the rat hippocampus. *Synapse* **62**, 944–949 (2008).

15. Aghazadeh Tabrizi, M., Baraldi, P. G., Borea, P. A. & Varani, K. Medicinal Chemistry, Pharmacology, and Potential Therapeutic Benefits of Cannabinoid CB2Receptor Agonists. *Chem. Rev.* **116**, 519–560 (2016).

16. Volkow, N. D., Baler, R. D., Compton, W. M. & Weiss, S. R. B. Adverse Health Effects of Marijuana Use. *N. Engl. J. Med.* **370**, 2219–2227 (2014).

17. McKallip, R. J. *et al.* Targeting CB2 cannabinoid receptors as a novel therapy to treat malignant lymphoblastic disease. *Blood* **100**, 627–634 (2002).

18. Aso, E. & Ferrer, I. CB2 Cannabinoid Receptor As Potential Target against Alzheimer's Disease. *Front. Neurosci.* **10**, 1–10 (2016).

19. Concannon, R. M., Okine, B. N., Finn, D. P. & Dowd, E. Differential upregulation of the cannabinoid CB2 receptor in neurotoxic and inflammation-driven rat models of Parkinson's disease. *Exp. Neurol.* **269**, 133–141 (2015).

20. Benito, C. *et al.* Cannabinoid CB 2 receptors in human brain inflammation. *Br. J. Pharmacol.* **153**, 277–285 (2008).

21. Benito, C. *et al.* A glial endogenous cannabinoid system is upregulated in the brains of macaques with simian immunodeficiency virus-induced encephalitis. *J. Neurosci.* **25**, 2530–2536 (2005).

22. Chakravarti, B., Ravi, J. & Ganju, R. K. Cannabinoids as therapeutic agents in cancer: Current status and future implications. *Oncotarget* **5**, 5852–5872 (2014).

23. Ellert-Miklaszewska, A., Ciechomska, I. & Kaminska, B. Cannabinoid signaling in glioma cells. *Adv. Exp. Med. Biol.* **986**, 209–220 (2013).

24. Pertwee, R. G. Targeting the endocannabinoid system with cannabinoid receptor agonists: Pharmacological strategies and therapeutic possibilities. *Philos. Trans. R. Soc. B Biol. Sci.* **367**, 3353–3363 (2012).

25. Savonenko, A. V. *et al.* Cannabinoid CB2 receptors in a mouse model of Aβ amyloidosis: Immunohistochemical analysis and suitability as a PET biomarker of neuroinflammation. *PLoS One* **10**, 1–23 (2015).

26. Slavik, R. *et al.* Development and evaluation of novel pet tracers for imaging cannabinoid receptor type 2 in brain. *Chimia (Aarau).* **68**, 208–210 (2014).

27. Haider, A. *et al.* Synthesis and biological evaluation of thiophene-based cannabinoid receptor type 2 radiotracers for PET imaging. *Front. Neurosci.* **10**, 1–10 (2016).

28. Slavik, R. *et al.* Discovery of a high affinity and selective pyridine analog as a potential positron emission tomography imaging agent for cannabinoid type 2 receptor. *J. Med. Chem.* **58**, 4266–4277 (2015).

29. Evens, N. *et al.* Preclinical evaluation of [11C]NE40, a type 2 cannabinoid receptor PET tracer. *Nucl. Med. Biol.* **39**, 389–399 (2012).

30. Slavik, R. *et al.* Synthesis, radiolabeling and evaluation of novel 4-oxo-quinoline derivatives as PET tracers for imaging cannabinoid type 2 receptor. *Eur. J. Med. Chem.* **92**, 554–564 (2015).

31. Horti, A. G. *et al.* Synthesis and biodistribution of [11C]A-836339, a new potential radioligand for PET imaging of cannabinoid type 2 receptors (CB2). *Bioorganic Med. Chem.* **18**, 5202–5207 (2010).

32. Moldovan, R. P. *et al.* Development of a High-Affinity PET Radioligand for Imaging Cannabinoid Subtype 2 Receptor. *J. Med. Chem.* **59**, 7840–7855 (2016).

33. Evens, N. *et al.* Synthesis, in vitro and in vivo evaluation of fluorine-18 labelled FE-GW405833 as a PET tracer for type 2 cannabinoid receptor imaging. *Bioorganic Med. Chem.* **19**, 4499–4505 (2011).

34. Vandeputte, C. *et al.* A PET brain reporter gene system based on type 2 cannabinoid receptors. *J. Nucl. Med.* **52**, 1102–1109 (2011).

35. Ahmad, R. *et al.* Whole-body biodistribution and radiation dosimetry of the cannabinoid type 2 receptor ligand [11C]-NE40 in healthy subjects. *Mol. Imaging Biol.* **15**, 384–390 (2013).

36. Ahmad, R. *et al.* Decreased in vivo availability of the cannabinoid type 2 receptor in Alzheimer's disease. *Eur. J. Nucl. Med. Mol. Imaging* **43**, 2219–2227 (2016).

37. Spinelli, F., Mu, L. & Ametamey, S. M. Radioligands for positron emission tomography imaging of cannabinoid type 2 receptor. *J. Label. Compd. Radiopharm.* **61**, 299–308 (2018).

38. Ghonim, A. E. *et al.* Structure-activity relationships of thiazole and benzothiazole derivatives as selective cannabinoid CB2 agonists with in vivo anti-inflammatory properties. *Eur. J. Med. Chem.* **180**, 154–170 (2019).

39. Spinelli, F., Capparelli, E., Abate, C., Colabufo, N. A. & Contino, M. Perspectives of Cannabinoid Type 2 Receptor (CB2R) Ligands in Neurodegenerative Disorders: Structure-Affinity Relationship (SAfiR) and Structure-Activity Relationship (SAR) Studies. *J. Med. Chem.* **60**, 9913–9931 (2017).

40. Parlati, Francesco; Ramesh, Usha V.; Singh, Rajinder; Payan, Donald G.; Lowe, R. L. G. Benzothiazole and thiazole[5,5-b] pyridine compositions and their use as ubiquitin ligase inhibitors. (2005).

41. Rühl, T. *et al.* Cannabinoid receptor type 2 (CB2) -selective N -aryl-oxadiazolyl-propionamides : synthesis , radiolabelling , molecular modelling and biological evaluation. *Org. Med. Chem. Lett.* **2**, 1–22 (2012).

42. Ritawidya, R., Ludwig, F., Briel, D., Brust, P. & Scheunemann, M. Synthesis and In Vitro Evaluation of 8-Pyridinyl-Substituted Benzo[e]imidazo[2,1-c][1,2,4]triazines as Phosphodiesterase 2A Inhibitors. *Molecules* **24**, 1–21 (2019).